Synthesis of Prepolymerization Stage in Polycondensation Processes

Ketan D. Samant and Ka M. Ng
Dept. of Chemical Engineering, University of Massachusetts, Amherst, MA 01003

A systematic design procedure of the prepolymerization stage of a polycondensation process is presented. This procedure treats polycondensation processes as reactive separation processes and offers an alternative to design through simulations. Feasible flowsheets and operating conditions are developed by analyzing the phase behavior of polycondensation systems at thermodynamic equilibrium. Functional end groups and apparent mole fractions are used to represent reaction kinetics and equilibrium, and real mole fractions are used to represent phase equilibrium. Reactive phase diagrams are plotted in transformed mole-fraction space to facilitate visualization of the phase behavior. Three examples are presented: manufacture of polyethylene terephthalate (PET) from dimethyl terephthalate (DMT) and ethylene glycol (EG), from terephthalic acid (TPA) and EG, and manufacture of nylon-6,6. For these processes, the results of the approach agree excellently with detailed iterative performance simulations. The approach also reveals additional feasible process alternatives and corresponding operating conditions.

Introduction

Many commercially important polymers, such as nylons, polyesters, and polycarbonates, are manufactured by polycondensation. Polycondensation processes are step-growth polymerization processes in which the reaction step is accompanied by the formation of a low-molecular-weight condensate. Design of polycondensation processes is a challenging problem (Ravindranath and Mashelkar, 1986a,b). To obtain a polymer product of high molecular weight, it is essential to maintain proper end-group stoichimetry, to remove the condensate byproduct in order to shift the reaction equilibrium, and to avoid degradation due to side reactions (Dotson et al., 1996; Gupta and Kumar, 1987; Jacobsen and Ray, 1992a,b). It is difficult to ensure these conditions throughout the polycondensation process for a number of reasons: disruption of end-group stoichiometry due to the loss of volatile monomer(s), the presence of multiple polycondensation routes, and the presence of monomers in different phases; loss of product due to the loss of volatile monomer(s); and difficulty in condensate removal due to limited rates of diffusion through the polymer and limited rates of interphase mass transfer; to cite a few. In order to overcome these difficulties, it is essential to make judicious choices about process equipment and operating conditions based on an understanding of the underlying physical and chemical processes.

Industrial polycondensation processes typically include up to three distinct process stages: prepolymerization, polymerization, and finishing (Figure 1). The prepolymerization stage is used to prepare a short-chain polymer that forms the feed to the polymerization and finishing stages. This is done in order to ensure that the stoichiometric and thermodynamic limitations do not propagate onto the polymerization and finishing stages where the bulk of polymerization takes place. For instance, in production of polyethylene terephthalate (PET) from dimethyl terephthalate (DMT) and ethylene glycol (EG), the prepolymerization stage is used to prepare bishydroxyethyl terephthalate (BHET) and its oligomers, which have inherent 1:1 end-group stoichiometry. In the production of PET from terephthalic acid (TPA) and EG, in addition to preparing BHET, the prepolymerization stage ensures complete dissolution of solid TPA. In the production of nylon-6, it is used to initiate the polymerization reaction by opening the ring monomer (ϵ-caprolactum), and in the production of nylon-6,6 it is used to minimize the loss of volatile monomer

Correspondence concerning this article should be addressed to K. M. Ng.

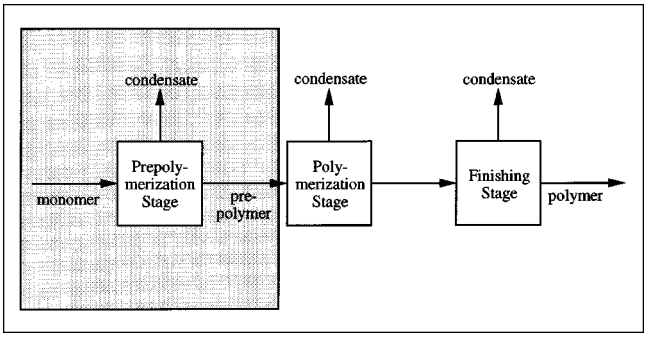

Figure 1. Three stages of polycondensation processes.

hexamethylene diamine (HMDA). Thus proper design of the prepolymerization stage is crucial for the success of the entire polycondensation process.

The goal of this article is to present a systematic procedure to synthesize feasible process alternatives for prepolymerization processes. This approach is based on equilibrium thermodynamics and treats polycondensation processes as reactive separation processes. We present our approach below by applying it to the production of PET from DMT and EG. We also demonstrate the utility of our approach with two additional commercially important examples: production of PET from TPA and EG, and production of nylon-6,6 from HMDA and adipic acid (AA).

Synthesis of Prepolymerization Processes

There are important differences between synthesis and simulation of chemical processes. In a simulation, the inputs, process flow sheet, and design variables are specified, and the aim is to calculate all of the outputs. On the other hand, in a synthesis problem, the inputs and desired process outputs are given, and the goal is to determine feasible process alternatives and design variables necessary to achieve them.

Frequently, a design problem is solved through successive simulations. After assuming a process flowsheet and base-case values for the design variables (operating conditions), these variables are improved through successive simulations till the design matches the desired specifications. This simulation approach has been followed for the design of the prepolymerization stage in most of the work done to date (Besnoin et al., 1989; Choi, 1987; Gupta and Kumar, 1987; Ravindranath and Mashelkar, 1981, 1982a,b,c). While it provides a feasible design, it can be time-consuming, as it involves a lot of trial-and-error runs. This is especially so since a lot of uncertainty typically exists in physical property values and models.

As an alternative to repeated simulations, our equilibrium thermodynamics-based procedure provides insights into feasible process alternatives and operating conditions. As summarized below, the procedure consists of four steps.

Step 1: Specifications
- (a) Input
- (b) Output
- (c) Constraints

Step 2: Representation of Phase and Reaction Equilibria
- (a) Representation of reaction kinetics
- (b) Phase and reaction equilibria
- (c) Reactive phase diagrams

Step 3: Feasible Process Flowsheets and Operating Conditions

Step 4: Comparison of Alternatives
- (a) Cost and Operability
- (b) Sensitivity

The details of each step and the design tools and calculations used at each stage are described below for the production of PET from DMT and EG (Example 1).

Step 1: Specifications

This step specifies the inputs to the process, the outputs desired from the process, the constraints we wish to impose on the operations, and the reasons behind these specifications. These specifications should be carefully chosen, as the feasible process alternatives and feasible ranges of operating conditions depend on them.

Step 1 for Example 1. The prepolymerization stage of this process involves transesterification of DMT with EG in the presence of homogeneous metal acetate catalyst. The desired product is BHET and its oligomers. The specifications for this process can be summarized as:

- Input specifications.

Raw materials are pure DMT and EG.

- Output specifications.

Desired product is BHET and its oligomers ($1.5 \leq DP_n \leq 5$, preferably $DP_n \approx 2.0$). Complete conversion of methyl ester end groups. Minimum loss of volatile raw materials (EG).

- Constraints.

Operating temperature should not exceed 573.15 K.

The reason for producing BHET and its oligomers, and ensuring complete conversion of methyl ester end groups, will become clearer when we consider the kinetic scheme in the next step. The objective of the prepolymerization stage is not chain buildup, but to prepare prepolymer that is suitable for chain buildup in the polymerization and finishing stages. Hence, the degree of polymerization is kept low ($1.5 \leq DP_n \leq 5$, preferably $DP_n \approx 2.0$) in order to avoid having to handle high viscosities. The upper limit on temperature is necessary to minimize the formation of undesired side products such as acetylene and diethylene glycol (DEG), which have an adverse influence on the polymer quality (Gupta and Kumar, 1987; Besnoin and Choi, 1989).

Step 2: Representation of phase and reaction equilibria

Step 2 concerns the representation of the phase behavior of a polycondensation process. Careful attention is given to the representation of kinetic schemes, description of phase and reaction equilibrium equations, and visualization of phase behavior using reactive phase diagrams. These issues are considered in more detail below.

Step 2a: Representation of Reaction Kinetics. The functional end-group representation (Gupta and Kumar, 1987) is used in our approach. In this representation, the kinetic scheme is written in terms of the functional end groups on the polymer species. These functional end groups represent the *apparent* reacting components (*real* components being monomers, condensate, and polymer chains) and their compositions are expressed in terms of *apparent* mole fractions

Table 1. Reaction Kinetics for Example 1

Representation of Kinetic Scheme		
1. Transesterification:	$E_m + EG \leftrightarrow E_g + M$	
2. Polycondensation I:	$E_m + E_g \leftrightarrow Z + M$	
3. Polycondensation II:	$E_g + E_g \leftrightarrow Z + EG$	
Catalyst: Homogeneous metal acetate catalyst		
EG: Ethylene glycol ($HO-CH_2CH_2-OH$) M: Methanol (CH_3OH) Z: Polymer linkage ($---\phi-COOCH_2CH_2OOC-\phi---$) E_m: Methyl ester end group ($---\phi-COOCH_3$) E_g: Hydroxyl ester end group ($---\phi-COOCH_2CH_2-OH$)		
Rate Expressions		
1. Transesterification:	$R_1 = k_1\left(2x_{E_m}x_{EG} - \frac{x_{E_g}x_M}{K_1}\right)$	
2. Polycondensation I:	$R_2 = k_2\left(x_{E_m}x_{E_g} - \frac{2x_Z x_M}{K_2}\right)$	
3. Polycondensation II:	$R_3 = k_3\left(x_{E_g}^2 - \frac{4x_Z x_{EG}}{K_3}\right)$	
Kinetic Parameters $k_i\ (1/\text{min}) = A_i \exp[-E_i/RT]$		
Reaction	A_i (1/min)	E_i (kcal/mol)
1. Transesterification	0.4552×10^6	15.0
2. Polycondensation I	0.2276×10^6	15.0
3. Polycondensation II	7.7384×10^6	18.5

(compositions of real components are expressed as *real* mole fractions). There are only a limited number of reactions in this representation, and the functional end groups can easily be incorporated into the phase and reaction equilibrium models. The major drawback is that the information about the second and higher moments of the chain length distribution is lost. Thus, we cannot estimate the polydispersity of the product. However, this is not a very significant drawback, as polydispersity for most polycondensation processes is close to the most probable value of 2.0 (Gupta and Kumar, 1987; Besnoin et al., 1989; Steppan, 1989), and it is not a major design concern (and hence not included in the specifications of Step 1) in the prepolymerization stage, as the majority of the chain buildup takes place in the polymerization and finishing stages.

Step 2a for Example 1. For this example, the kinetic scheme can be represented in terms of the functional end groups as shown in Table 1. The table also lists the rate expressions and rate constants for the reaction mechanisms. It should be noted that these rate expressions are written in terms of apparent mole fractions and not in terms of concentrations so as to be consistent with the phase and reaction equilibrium models and to yield rate constants with units of reciprocal time. The rate constants are regressed from the end-group concentration-based rate constants available in the literature (Gupta and Kumar, 1987).

Only two of the three reactions listed in Table 1 are independent at equilibrium. The chain buildup takes place through two routes: polycondensation I and polycondensation II. Polycondensation I is a reaction between two different functional end groups, and polycondensation II is a reaction between similar end groups. Hence polycondensation II is inherently stoichiometrically balanced, whereas polycondensation I is not. We would not have to worry about end-group stoichiometry if the chain buildup took place only through polycondensation II. This is the reason why we wanted to produce BHET and its oligomers (which have hydroxyl ester end groups on both chain ends) and ensure complete conversion of methyl ester end groups.

In the representation of Table 1, we considered only the main reactions. Some side reactions also take place (Ravindranath and Mashelkar, 1986a). However, these reactions are not included in our analysis, as reliable information on their mechanisms, rate expressions, and kinetic parameters is not available. The side reactions can easily be included in our analysis if this information is available. Here, we account for these side reactions by imposing the temperature constraint. Fine-tuning of operating conditions may be done for the selected process alternatives to ensure minimum production of undesired side products.

Step 2b: Phase and Reaction Equilibria. A polycondensation system of c apparent components in p phases undergoing r independent chemical reactions, satisfies $c(p-1)$ phase equilibrium and r reaction equilibrium equations at thermodynamic equilibrium. In this step, reaction equilibrium is described by expressing the reaction equilibrium constants as functions of activities (or mole fractions) of reacting components. Typically, polycondensation systems exhibit only two phases (vapor and liquid). Vapor-liquid (VLE) equilibrium is described using the Flory-Huggins theory. All polymeric species are assumed to be nonvolatile. In case an additional solid or liquid phase exists, appropriate solid–liquid equilibrium (SLE) or liquid–liquid equilibrium (LLE) models are used in conjunction with the Flory-Huggins equations.

The reaction equilibrium equations are written in terms of apparent mole fractions, while the phase equilibrium equations are written in terms of real mole fractions. Hence to make the reaction and phase-equilibrium equations consistent, relationships between real and apparent mole fractions are also developed in this step.

Step 2b for Example 1. The equilibrium constants for the three reactions of Table 1 are written in terms of the apparent mole fractions as

$$K_1 = \frac{x_{E_g}x_M}{2x_{E_m}x_{EG}} \tag{1a}$$

$$K_2 = \frac{2x_Z x_M}{x_{E_m}x_{Eg}} \tag{1b}$$

$$K_3 = \frac{K_2}{K_1} = \frac{4x_Z x_{EG}}{x_{E_g}^2}. \tag{1c}$$

The values of these equilibrium constants are listed in Table 2.

EG and methanol (M) are considered to be the only volatile components of the reaction mixture. The VLE relationship is given by

$$Py_i = P_i^0\gamma_i\phi_i, \qquad i = \text{EG, M,} \tag{2}$$

where the activity coefficients are given by the Flory-Huggins

Table 2. Thermodynamic Parameters for Example 1

Reaction Equilibrium Constants
$K_1 = 0.3$
$K_2 = 0.15$
$K_3 = \dfrac{K_2}{K_1} = 0.5$
Vapor Pressure Correlations
$\log P^0_{\mathrm{EG}}\ (\mathrm{Pa}) = 11.521 - \dfrac{3{,}066.5}{\mathrm{T(K)}}$
$\log P^0_{\mathrm{M}}\ (\mathrm{Pa}) = 10.541 - \dfrac{1{,}867.9}{\mathrm{T(K)}}$
Molar Volume Correlations
$\nu_{\mathrm{EG}}(cm^3/mol) = 60.6[1 + 0.0014(\mathrm{T(K)} - 413)]$
$\nu_{\mathrm{M}}(cm^3/mol) = 43.5[1 + 0.0014(T(\mathrm{K}) - 413)]$
$\nu_{\mathrm{poly}}(cm^3/mol) \cong 191.5[1 + 0.0014(T(\mathrm{K}) - 413)]$

theory as

$$\gamma_i = \exp\left[\left(1 - \frac{1}{DP_n}\right)\phi_{\mathrm{poly}} + \chi_i \phi^2_{\mathrm{poly}}\right], \qquad i = \mathrm{EG, M,} \quad (3)$$

χ_i is the polymer-solvent interaction parameter. Vrentas et al. (1983) found this parameter to be in the range of 0.3–0.5 for most polymer–solvent systems. Here (and also for the remaining examples), we will take it to be equal to 0.5. The vapor pressures of EG and methanol are listed in Table 2 as functions of temperature. The degree of polymerization (DP_n) in Eq. 3 is given by

$$DP_n = \frac{\mu_1}{\mu_0}, \quad (4)$$

where, μ_0 and μ_1 are the zeroth and the first moments of the chain-length distribution; μ_0 represents the number of moles of polymer chains, and μ_1 represents the number of moles of monomer units in these chains. By noting that any polymer chain containing (n) monomer units has two end groups and ($n-1$) polymer linkages, we can write:

$$\mu_0 = \frac{\left(N_{\mathrm{E_g}} + N_{\mathrm{E_m}}\right)}{2} \quad (5a)$$

$$\mu_1 - \mu_0 = N_Z. \quad (5b)$$

Here N_i is the number of moles of species i. If we substitute Eq. 5 into Eq. 4, after some algebraic manipulation we can write the degree of polymerization in terms of the apparent mole fractions as:

$$DP_n = 1 + \frac{2x_Z}{\left(x_{\mathrm{E_g}} + x_{\mathrm{E_m}}\right)}. \quad (6)$$

For this example, the real components in the reaction mixture are EG, methanol, and polymer chains (DMT is considered as a polymeric species). The volume fractions of these species in the reaction mixture can be written as

$$\phi_{\mathrm{EG}} = \frac{\nu_{\mathrm{EG}}\hat{x}_{\mathrm{EG}}}{\left(\nu_{\mathrm{EG}}\hat{x}_{\mathrm{EG}} + \nu_{\mathrm{M}}\hat{x}_{\mathrm{M}} + \nu_{\mathrm{poly}}\hat{x}_{\mathrm{poly}}\right)} \quad (7a)$$

$$\phi_{\mathrm{M}} = \frac{\nu_{\mathrm{M}}\hat{x}_{\mathrm{M}}}{\left(\nu_{\mathrm{EG}}\hat{x}_{\mathrm{EG}} + \nu_{\mathrm{M}}\hat{x}_{\mathrm{M}} + \nu_{\mathrm{poly}}\hat{x}_{\mathrm{poly}}\right)} \quad (7b)$$

$$\phi_{\mathrm{poly}} = 1 - \phi_{\mathrm{EG}} - \phi_{\mathrm{M}} = \frac{\nu_{\mathrm{poly}}\hat{x}_{\mathrm{poly}}}{\left(\nu_{\mathrm{EG}}\hat{x}_{\mathrm{EG}} + \nu_{\mathrm{M}}\hat{x}_{\mathrm{M}} + \nu_{\mathrm{poly}}\hat{x}_{\mathrm{poly}}\right)}, \quad (7c)$$

where ν_{EG}, ν_{M}, and ν_{poly} are the molar volumes of EG, methanol, and polymeric species, respectively (also listed in Table 2), and $\hat{x}_{\mathrm{EG}}$, $\hat{x}_{\mathrm{M}}$, and $\hat{x}_{\mathrm{poly}}$ are the real mole fractions for the reaction mixture. The total moles of real species in the mixture is given by

$$\hat{N}_T = \hat{N}_{\mathrm{EG}} + \hat{N}_{\mathrm{M}} + \hat{N}_{\mathrm{poly}} = \hat{N}_{\mathrm{EG}} + \hat{N}_{\mathrm{M}} + \frac{\left(N_{\mathrm{E_g}} + N_{\mathrm{E_m}}\right)}{2}. \quad (8)$$

Here $\hat{N}_i$ represents the number of moles of real species i. By noting that $\hat{N}_{\mathrm{EG}} = N_{\mathrm{EG}}$, and $\hat{N}_{\mathrm{M}} = N_{\mathrm{M}}$, we can rewrite the previous equation as

$$\hat{N}_T = N_{\mathrm{EG}} + N_{\mathrm{M}} + \frac{\left(N_{\mathrm{E_g}} + N_{\mathrm{E_m}}\right)}{2}. \quad (9)$$

Also,

$$N_T = N_{\mathrm{EG}} + N_{\mathrm{M}} + N_{\mathrm{E_g}} + N_{\mathrm{E_m}} + N_Z. \quad (10)$$

Using these equations, the real mole fractions can be written as

$$\hat{x}_{\mathrm{EG}} = \frac{N_{\mathrm{EG}}}{\hat{N}_T} = \frac{N_{\mathrm{EG}}/N_T}{\hat{N}_T/N_T} = \frac{x_{\mathrm{EG}}}{\left[1 - x_Z - \left(x_{\mathrm{E_g}} + x_{\mathrm{E_m}}\right)/2\right]} \quad (11a)$$

$$\hat{x}_{\mathrm{M}} = \frac{x_{\mathrm{M}}}{\left[1 - x_Z - \left(x_{\mathrm{E_g}} + x_{\mathrm{E_m}}\right)/2\right]} \quad (11b)$$

$$\hat{x}_{\mathrm{poly}} = \frac{\left[\left(x_{\mathrm{E_g}} + x_{\mathrm{E_m}}\right)/2\right]}{\left[1 - x_Z - \left(x_{\mathrm{E_g}} + x_{\mathrm{E_m}}\right)/2\right]}. \quad (11c)$$

These relationships between real and apparent mole fractions complete the description of phase and reaction equilibria for Example 1. It should be noted that both real and apparent mole fractions add up to unity.

Step 2c: Reactive Phase Diagrams. To develop feasible process flowsheets, we need to visualize the behavior of the system at phase and reaction equilibrium. Here the reacting system has five apparent components. Hence, it is impossible to plot the phase diagram for this system. However, the dimensionality of the system can be reduced by using the trans-

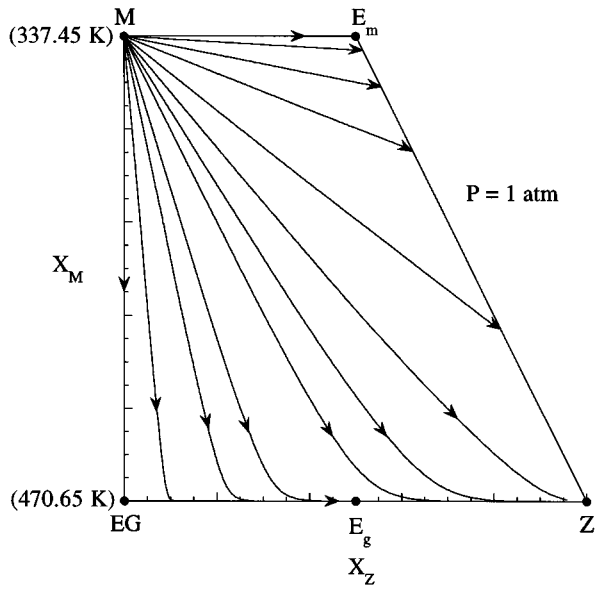

Figure 2. Residue curve map at atmospheric pressure for Example 1.

formed mole-fraction coordinates developed by Ung and Doherty (1995a).

In the transformed coordinate space, all the compositions shown on the phase diagram are those on the reaction equilibrium surface. This reduces the number of independent variables of the system by the number of reactions without any loss of information. Phase diagrams plotted in the transformed coordinate space are called reactive phase diagrams. Reactive phase diagrams have been extensively used for equilibrium analysis and synthesis of reactive separation processes, for example, reactive distillation (Ung and Doherty, 1995b), reactive crystallization (Berry and Ng, 1997), and extractive reaction (Samant and Ng, 1998a).

Step 2c for Example 1. For our example, with E_g and E_m as reference components, the transformed mole fraction coordinates are

$$X_{EG} = x_{EG} + \frac{x_{E_g}}{2} - \frac{x_{E_m}}{2} \tag{12a}$$

$$X_M = x_M + x_{E_m} \tag{12b}$$

$$X_Z = 1 - X_{EG} - X_M = x_z + \frac{x_{E_g}}{2} + \frac{x_{E_m}}{2}. \tag{12c}$$

The reactive phase diagram is as shown in Figure 2. The EG–M, E_m–M, and E_m–Z edges are the nonreactive edges. Any composition on these edges corresponds to a nonreactive mixture. The EG–E_g–Z edge is the reactive edge. Any composition on this edge corresponds to a reactive mixture of EG and polymer chains with hydroxyl ester end groups at equilibrium. Any composition within the phase diagram corresponds to a reactive mixture at equilibrium that contains all five components. EG and methanol are the only volatile components. Hence the vapor composition is constrained to lie on the EG–M nonreactive edge. The liquid composition can lie anywhere on the phase diagram. Note that material balance equations with or without reactions can be represented as straight lines on the reactive phase diagram (Samant and Ng, 1998a).

Figure 2 also shows the residue curve map for $P = 1$ atm. The map shows that the system does not possess azeotropes, reactive distillation boundaries, and tangent pinches. The residue curves emanate from the lightest component methanol (stable node) and end either on the Z and E_m vertices (stable nodes) or on some composition on the $E_m - Z$ nonreactive edge. The EG vertex is a saddle. The $E_m - Z$ edge represents a nonvolatile mixture composed entirely of polymeric species. This is the reason the residue curves seem to end on all points on this edge (instead of ending only on vertex Z or on vertex E_m). Interestingly, the absence of azeotropes and distillation boundaries can be deduced without plotting the residue curves, as shown in the Appendix.

Step 3: Feasible process flowsheets and operating conditions

In Step 3, we analyze the phase behavior to develop feasible process flowsheets and corresponding operating conditions to attain the design specifications.

Operating Conditions. The important operating conditions that are considered are the molar ratio of monomers in the feed (feed composition), pressure, and temperature ranges, and the average residence time (or molar holdup). Feed ratio and range of operating temperature are typically fixed on the basis of the desired degree of polymerization. Operating pressure is fixed by the economic desirability of being able to condense the lightest component of the reaction mixture by using cooling water from cooling towers (Douglas, 1988). It should be noted that these are not the only criteria used to determine feed ratio and pressure and temperature ranges. The determination of these operating conditions depends strongly on the specifications and the phase behavior of the system under consideration.

Our analysis of phase behavior is based on the assumption that the reacting system is at phase and reactive equilibrium. In reality, the system can be kinetically controlled. Consider a multiphase reactive separator with r reactions. If we write detailed material balance equations at constant temperature and pressure, the approach to reaction equilibrium can be shown to be governed by dimensionless Damköhler numbers (Venimadhavan et al., 1994; Nisoli et al., 1997; Samant and Ng, 1998b) defined as

$$Da_i = k_i \tau \qquad i = 1, 2, \ldots, r. \tag{13}$$

Here, k_i is the forward reaction rate constant of reaction i, and τ is the residence time. Damköhler number Da_i measures the rate of reaction i relative to the rate of product removal. Typically a reaction is extremely close to equilibrium for $Da \gg 1$. For our design calculations, we use $Da = 1$ to determine the lower bound on average residence time in the reactive zone at the operating pressure and temperature. This lower bound is estimated as

$$\tau_{\min} = \left(\min_{i = 1, 2, \ldots, r} k_i \right)^{-1}. \tag{14}$$

The average residence times used should be much in excess of the lower bound. The preceding equation can be equivalently used for determining lower bounds on molar holdups in reactive zones if molar flow rates are known.

Rigorous modeling and optimization can be done once a flowsheet has been selected for further development. The operating conditions as determined earlier can be used as the basis for modeling and optimization.

Feasible Process Flowsheets. Let us focus on the prepolymerization stage as enclosed in the shaded region in Figure 1. Monomers are fed to the stage in the desired molar ratio. We want to remove the condensate as a byproduct and the prepolymer as the main product of the stage. This can be achieved by using one of the four basic reaction-separation flowsheet configurations shown in Figure 3. In this figure (and also in rest of the flow sheets) the reactive zones are indicated by the shaded regions.

A continuous stirred-tank reactor (CSTR) with separator (Figure 3a) is the simplest configuration for a reactive separation process. Reaction occurs in the CSTR. The condensate is removed in the separator and the recovered volatile monomer(s) is(are) recycled back to the reactor. In Figure 3b, the CSTR is replaced with a cascade of CSTRs operating at different temperatures and pressures. The prepolymer is removed from the last reactor and monomer(s) is(are) recycled to the first reactor. A cascade of CSTRs is equivalent to a plug-flow reactor (PFR), as the number of reactors in the cascade tends to infinity with the molar holdup within each reactor tending to zero. Hence, we can replace the cascade of CSTRs in Figure 3b with a PFR, as shown in Figure 3c. Temperature and pressure profiles have to be maintained along the length of the PFR. A reactive separator (Figure 3d) combines the reaction and separation operations into one unit. The feasibility of reactive separation depends on the phase behavior of the system. If feasible, it reduces the number of process equipment and can substantially reduce the separator size.

Note that the preceding four configurations are not the only feasible configurations, but they form the building blocks for development of other feasible configurations. More complex configurations can be developed by changing stream destinations, by adding similar process units, and by combining two or more configurations. These modifications are made in order to make the process feasible, economical, and easy to operate in the desired range of operating conditions.

Step 3 for Example 1: Pressure. The bubble point of the lightest component (methanol) at atmospheric pressure is 337.45 K (147.74°F). Hence, we will operate our process at atmospheric pressure, as methanol can easily be condensed using cooling water.

Feed Ratio. Fresh feed to the process is a mixture of DMT and EG, and methanol (condensate) and the prepolymer form the products. We want prepolymer product with DP_n of about two and that does not contain any unreacted methyl ester end groups, that is, prepolymers that lie on the $EG-E_g-Z$ edge of the reactive phase diagram. Depending on the ratio of EG to DMT in the feed stream, the feed composition will

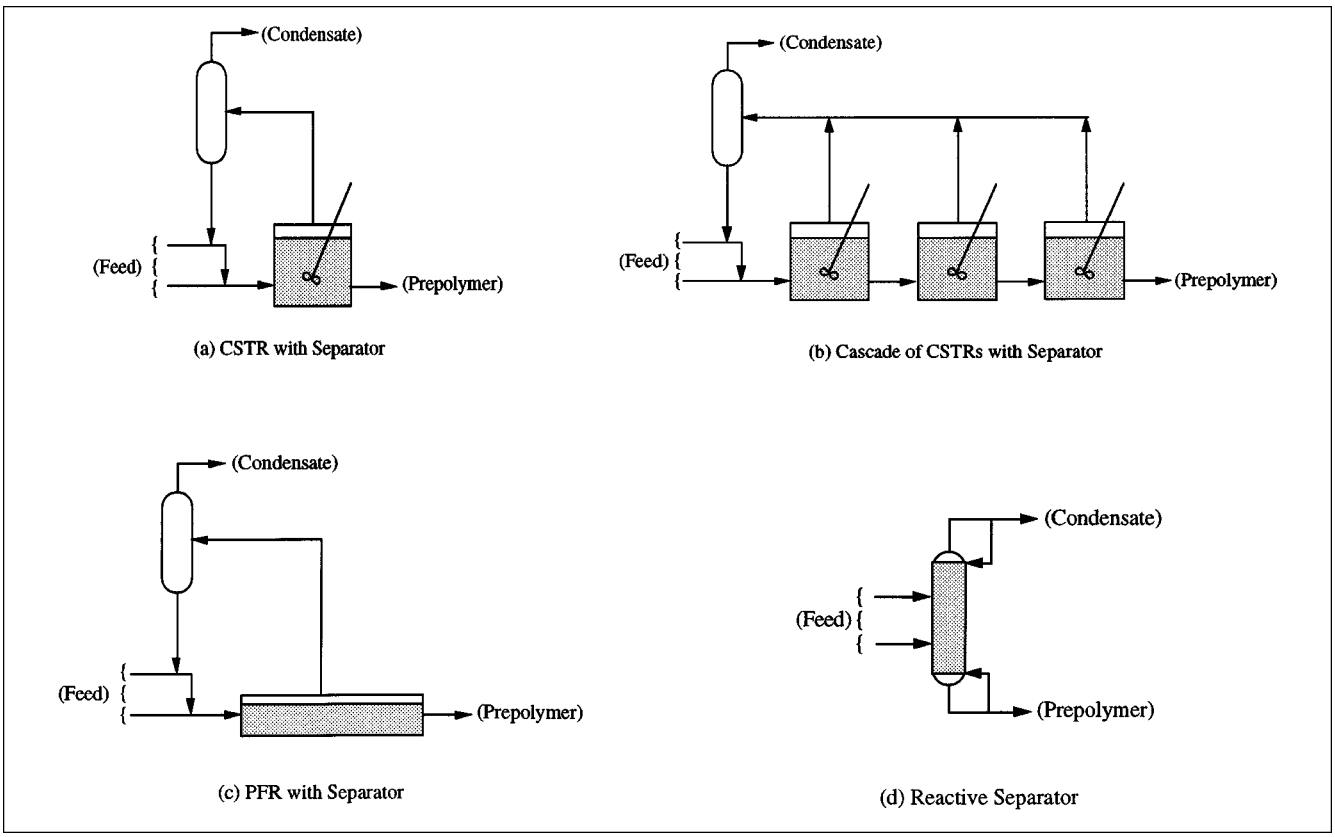

Figure 3. Basic flowsheet configurations for prepolymerization processes.

lie somewhere on line E_m–EG on the reactive phase diagram (Figure 4a). Material balance about the box of Figure 1 indicates that the feed, methanol, and prepolymer compositions should lie on a straight line on the reactive phase diagram. Hence, for the prepolymer composition to lie on the EG–E_g–Z edge, the feed composition should lie on line EG–F (the portion of line E_m–EG within the shaded region).

The EG–E_g–Z edge of the reactive phase diagram represents a three-component reactive mixture with one reaction (polycondensation II). According to the Gibbs phase rule, this system has $3(c)-1(r)-2(p)+2=2(f)$ degrees of freedom. Hence the composition (and hence DP_n) and temperature of the prepolymer product is fixed for a specified pressure and location on the EG–E_g–Z edge (that is, X_Z). In other words, at the specified pressure, every location on this edge has a temperature and degree of polymerization associated with it.

The location of the product on the EG–E_g–Z edge depends on the feed ratio. For example, in Figure 4a, the prepolymer composition would correspond to point P1 for feed composition corresponding to F1 and to point P2 for feed composition corresponding to F2. Hence, we can plot the degree of polymerization associated with a location on the EG–E_g–Z edge against the feed ratio required to reach that location as shown in Figure 4b. For the EG to DMT ratio of unity, the feed composition corresponds to point F, and the prepolymer composition corresponds to vertex Z ($DP_n \to \infty$). As this ratio increases, the prepolymer composition moves toward vertex EG ($DP_n = 1$). We need the EG to DMT ratio in the fresh-feed stream to be in the range 1.23 to 2.33 for $1.5 \le DP_n \le 5$ (Figure 4b); and $DP_n \approx 2$ when this ratio is 1.75. We will use this value in the rest of the discussion.

Temperature Range. At $P = 1$ atm, we can also plot the degree of polymerization associated with a location on the

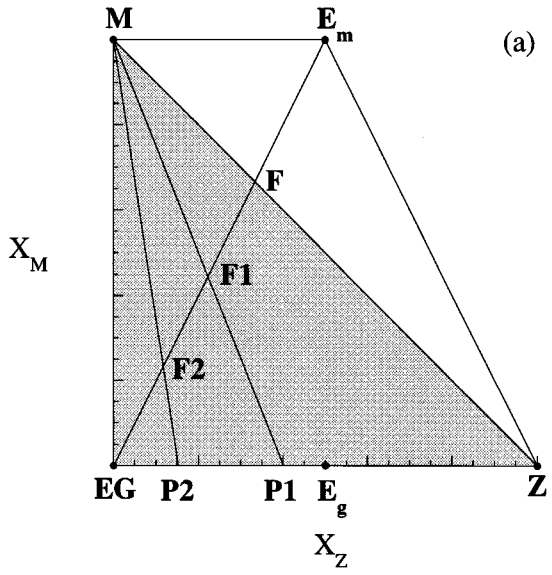

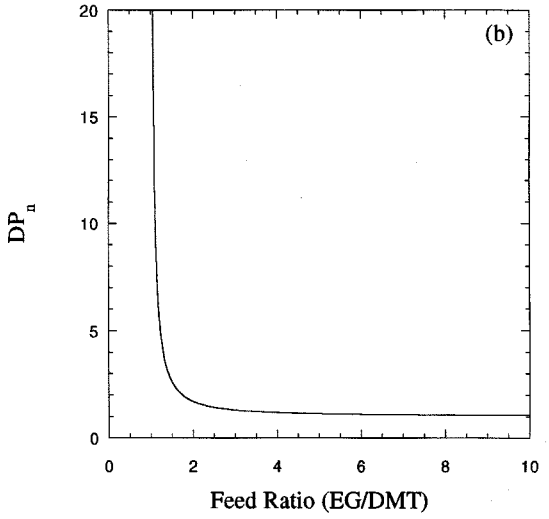

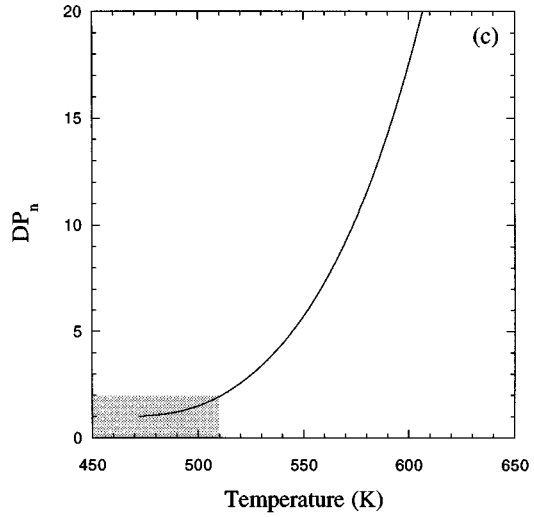

Figure 4. (a) Feasible feed ratios for Example 1; (b) degree of polymerization as a function of feed ratio for Example 1; (c) temperature as a function of degree of polymerization for Example 1.

For $DP_n \le 2.0$, operating temperature should lie within the shaded region. The maximum allowable temperature is 510 K.

$EG-E_g-Z$ edge against temperature as shown in Figure 4c. For $DP_n < 2$ (shaded region), the operating temperature has to be less than 510 K. Note that this upper bound does not violate the temperature constraint.

The lower bound on temperature is the bubble point of the lightest component at the selected operating pressure. At atmospheric pressure, methanol boils at 337.45 K. Hence 337.15 K–510 K forms the operating temperature range for this example.

Feasible Process Flowsheets: CSTR with Separator. The flowsheet and reactive phase diagram for a CSTR with separator are shown in Figure 5a. The stream numbers on the flowsheet correspond to the stream numbers on the phase diagram. At atmospheric pressure, EG and methanol can be completely separated in one distillation column. Within the temperature range of operation, the performance of this configuration at atmospheric pressure and feed ratio of 1.75 is shown in Figure 5b. At lower temperatures, the conversion of methyl ester end groups is unacceptably low, that is, the prepolymer product is far from the $EG-E_g-Z$ edge. The conversion increases as the temperature increases. However, this is accompanied by a very sharp increase in the amount of EG in the recycle stream. This increase corresponds to an increase in the sizes of the CSTR and the separator and represents wasteful utilization of energy for vaporizing and condensing EG. Thus, operating the CSTR at higher temperatures is not practical as the sizes of the CSTR and the distillation column needed are unacceptably high. Hence, though feasible, this configuration is unattractive from a practical standpoint.

Cascade of CSTRs with Separator. The preceding problem can be alleviated by increasing the temperature in steps by using a cascade of CSTRs. Initially, we want to keep as much EG in the liquid phase as possible by keeping the temperature low. As we move on, however, we also want to ensure near complete conversion of the methyl ester end groups by progressively increasing the temperature.

Figure 6 shows a flowsheet that uses a cascade of three CSTRs and corresponding reactive phase diagram. Typically, three reactors in series are sufficient to attain the desired specifications. The third reactor is operated at 510 K (the upper bound on temperature), and the first reactor at 470 K ($\sim$ the bubble point of EG at atmospheric pressure). The middle reactor is operated at an intermediate temperature of 490 K. The conversion of methyl ester end groups for this process (for the operating conditions of Figure 6) is 99.93%, and the ratio of EG in recycle stream to EG in fresh feed is only 1.41. In comparison, for a single CSTR operating at 510 K giving the same conversion, the ratio of EG in recycle stream to EG in fresh feed is 38.32.

PFR with Separator. The cascade of CSTRs can in principle be replaced with a PFR. In practice, however, it is difficult to maintain an increasing temperature profile and ensure vapor removal all along the length of a PFR. Hence, this configuration is unattractive from an operability point of view. In recent years, however, reactors with special internals that approximate plug flow have been developed (Schaeffer, 1995).

Reactive Distillation Column. The flowsheet and reactive phase diagram for a reactive distillation column are shown in Figure 7a. DMT is nonvolatile and is fed (with the catalyst) near the top of the column where it reacts with and hence

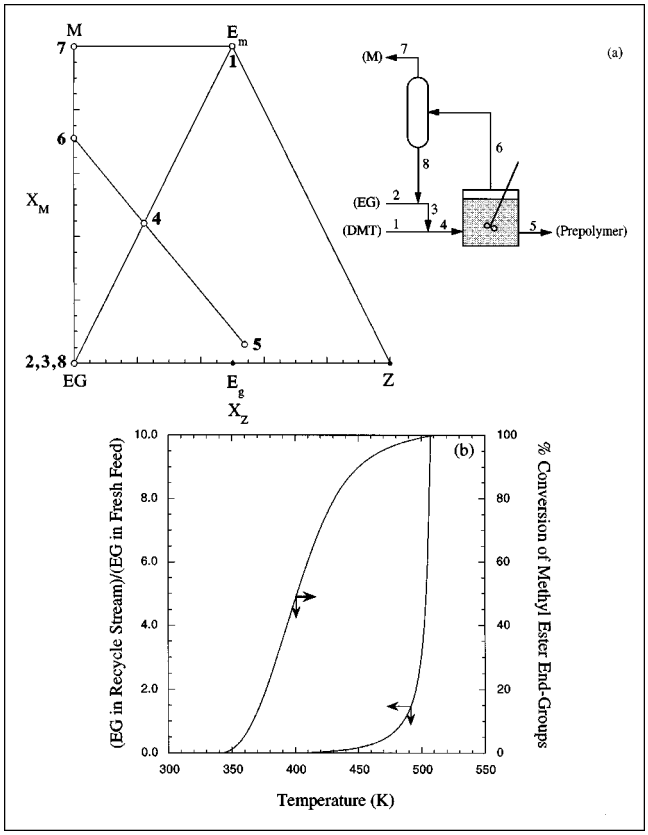

Figure 5. (a) Flowsheet and reactive phase diagram for CSTR with separator: $T = 510$ K, $P = 1$ atm; (b) performance of the CSTR with separator: trade-off between conversion and EG reflux.

facilitates the separation of EG. EG is fed near the bottom of the column. The overhead product is methanol and the bottoms product is the prepolymer. The temperature at the top of the column is 337.5 K (bubble point of methanol) and at the bottom is 510 K (upper bound on temperature). The temperature at the feed plate where molten DMT is introduced is higher than its melting point (preferably between 423.15 K and 448.15 K).

This operation is feasible, as the reactive mixture has no azeotropes and distillation boundaries at atmospheric pressure. The $M-EG-E_g-Z$ edges of the reactive phase diagram form a limiting residue curve (see Figure 2). Thus, if methanol is removed as the top product, any composition on the $EG-E_g-Z$ reactive edge can be removed as the bottom product of the prepolymerization process.

Reactive Distillation Column Fed Through Reboiler. In the reactive distillation column of Figure 7a, DMT is fed near the top of the column where the temperature is around 425 K. Hence initially the reaction takes place at temperatures much lower than the maximum allowable (510 K). In a variation of the configuration of Figure 7a, the distillation column can be fed through the reboiler as shown in Figure 7b. The reactive phase diagram for this configuration is also shown in Figure 7b. This configuration is arrived at by changing the stream destinations in Figure 7a. The reboiler is a CSTR that feeds the column. The overhead product is methanol and the

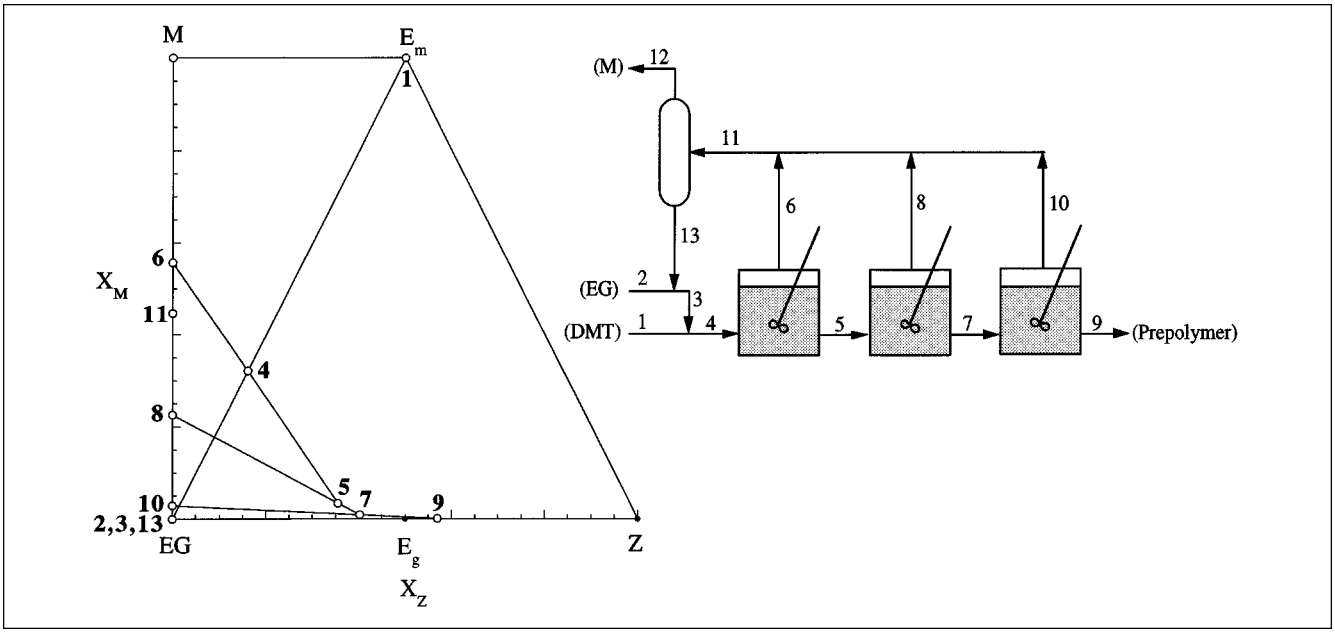

Figure 6. Flowsheet and reactive phase diagram for cascade of CSTRs with separator: $T_1 = 470$ K, $T_2 = 490$ K, $T_3 = 510$ K, $P = 1$ atm.

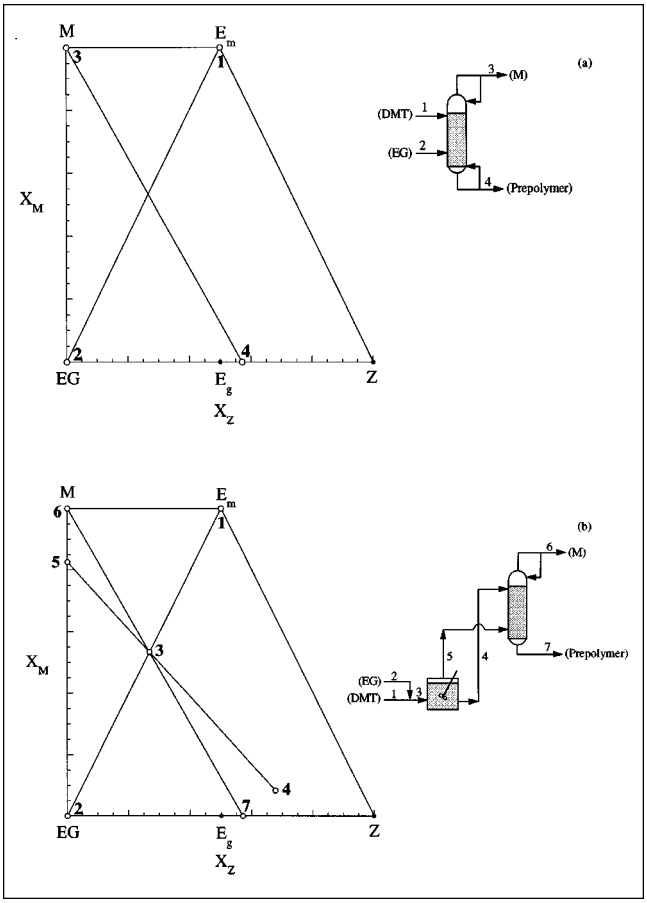

Figure 7. Flowsheet and reactive phase diagram for: (a) reactive distillation column; (b) reactive distillation column fed through reboiler.

prepolymer is taken out from the last plate of the column. The temperature at the top of the column is 337.5 K, and the temperature on the last plate is 510 K. The reboiler is also operated at 510 K.

The advantage here is that the reaction occurs initially at the highest possible temperature. This can potentially reduce the column diameter and height, that is, molar holdups and number of stages in the reactive distillation column.

Residence Time. Lower bounds on residence time are determined from Eq. 14 by using the reaction-rate constants listed in Table 1. For the CSTR cascade of Figure 6, the average residence times for the first, second, and third reactors should be greater than 51.83 min, 23.09 min, and 11.78 min, respectively. Residence times (or equivalently, molar holdups) for other feasible configurations can be similarly estimated.

Step 4: Comparison of alternatives

Step 4 deals with comparison of alternatives. While this step is not considered in detail in this article, the alternatives developed for Example 1 are assessed qualitatively in the preceding discussion on the basis of economics and operability. Shortcut cost models should be used for economic evaluation and sensitivity analysis of feasible process flowsheets.

Summary and Comparison with Simulation of Results for Example 1. Table 3 presents a summary of the feasible process flowsheets developed for Example 1 and corresponding operating conditions. Literature references to some of the configurations are also listed. It should be noted that these configurations and operating conditions were determined from the equilibrium-phase behavior, without having to perform repeated simulations.

Ravindranath and Mashelkar carried out a study of the prepolymerization process for this example using repeated

Table 3. Summary of Results for Example 1

Feasible Process Alternatives		
1. Cascade of CSTRs with separator (Gupta and Kumar, 1987; Ravindranath and Mashelkar, 1986a)		
2. Reactive distillation column (Bhatia, 1995; Vodonik, 1958)		
3. Reactive distillation column fed through reboiler		
*Feasible Operating Conditions and Comparison with Results of Repeated Simulations**		
Oper. Condition	Our Approach	Repeated Simul.
Feed ratio (EG/DMT)	1.75	1.3 to 1.9
Pressure	1 atm	1 atm
Temperature range	470 K to 510 K	453.15 K to 513.15 K
Residence time (for a 3 CSTR cascade)	$\tau_1 > 51.83$ min $\tau_2 > 23.09$ min $\tau_3 > 11.78$ min	$\tau_1 = 90$ min $\tau_2 = 60$ min $\tau_3 = 30$ min
Comparison with Simulation for a Cascade of Three CSTRs with Separator		
Specification	Desired	For Oper. Cond. Determined Above
DP_n of prepolymer product	2.0	1.996
x_{E_m} in prepolymer product	0.0	8.1138×10^{-4}
x_M in prepolymer product	0.0	1.2199×10^{-4}
Reactor temperature	< 573.15 K	453.15 K to 513.15 K

*Ravindranath and Mashelkar (1981, 1982a); Gupta and Kumar (1987).

Table 4. Reaction Kinetics for Example 2

Representation of Kinetic Scheme	
1. Esterification	$E_a + EG \leftrightarrow E_g + W$
2. Polycondensation I:	$E_a + E_g \leftrightarrow Z + W$
3. Polycondensation II:	$E_g + E_g \leftrightarrow Z + EG$
Catalyst: Antimony triacetate (homogeneous) and acid end groups	
EG: Ethylene glycol ($HO-CH_2CH_2-OH$)	
W: Water (H_2O)	
Z: Polymer linkage ($---\phi-COOCH_2CH_2OOC-\phi---$)	
E_a: Acid end group ($---\phi-COOH$)	
E_g: Hydroxyl ester end group ($---\phi-COOCH_2CH_2-OH$)	
Rate Expressions	
1. Esterification:	$R_1 = k_1\left(2x_{E_a}x_{EG} - \frac{x_{E_g}x_w}{K_1}\right)$
2. Polycondensation I:	$R_2 = k_2\left(x_{E_a}x_{E_g} - \frac{2x_Z x_w}{K_2}\right)$
3. Polycondensation II:	$R_3 = k_3\left(x_{E_g}^2 - \frac{4x_Z x_{EG}}{K_3}\right)$

Kinetic Parameters
k_i (1/min) = $A_i \exp[-E_i/RT]$

Reaction	A_i (1/min)	E_i (kcal/mol)
1. Esterification	11.8352×10^6	17.6
2. Polycondensation I	11.8352×10^6	17.6
3. Polycondensation II	7.7384×10^6	18.5

simulations of a semibatch reactor (1981) and a cascade of CSTRs with separator (1982a). Gupta and Kumar (1987) presented a preliminary optimization study for a semibatch process. A summary of the optimum operating conditions determined in these studies is also presented in Table 3 for the purpose of comparison. The operating conditions determined by our approach are in excellent agreement with those determined through repeated performance simulations. Once a flowsheet alternative is chosen for further development, operating conditions such as temperature distributions and residence times can be used as design variables for rigorous optimization.

The specifications of the products obtained from a feasible flowsheet configuration can be different from the desired specifications due to some approximations made in the design approach. To assess the accuracy of our approach, the cascade of CSTRs with separator was simulated with the operating conditions previously determined. A comparison of product specifications with desired specifications is also provided in Table 3. The results are in good agreement.

Additional Examples

In this section, we consider two additional examples to illustrate the procedure: production of PET from TPA and EG (Example 2), and production of nylon-6,6 from HMDA and AA (Example 3).

Example 2: Production of PET from TPA and EG

Step 1: Specifications. The prepolymerization stage involves direct esterification of TPA with EG in the presence of a homogeneous catalyst. Again, the desired product is BHET and its oligomers. The important difference here is that the TPA feed is in solid phase. The specifications for this example can be summarized as follows:

- Input specifications
  Raw materials are pure TPA(s) and EG.
- Output specifications
  Desired product is BHET and its oligomers ($1.5 \le DP_n \le 5$, preferably $DP_n \approx 2.0$).
  Complete dissolution of solid TPA.
  Complete conversion of acid end groups.
  Minimum loss of volatile raw materials (EG).
- Constraints
  Operating temperature should not be less than 513.15 K (240°C).
  Operating temperature should not exceed 573.15 K.

The reasons behind these specifications are the same as for the previous example. Here, we also want to ensure complete and early dissolution of solid TPA. This is necessary in order to obtain near complete conversion of acid end groups and to avoid the difficulty of handling solids in the polymerization and finishing stages. The lower limit on the reaction temperature comes about due to the fact that the reactions do not progress appreciably for temperatures less than 240°C (Katz, 1977).

Step 2a: Representation of Kinetic Scheme. The major reactions involved can be written in terms of functional end groups as shown in Table 4. Here again, we account for the side reactions through the temperature constraint. The rate expressions and kinetic parameters are also listed in Table 4. The kinetic parameters are regressed from concentration-based parameters available in the literature (Gupta and Kumar, 1987).

Step 2b: Phase and Reaction Equilibria. The equilibrium constants for the three reactions of Table 4 can be written in

Table 5. Thermodynamic Parameters for Example 2

Reaction Equilibrium Constants

$$K_1 = 2.5$$
$$K_2 = 1.25$$
$$K_3 = \frac{K_2}{K_1} = 0.5$$

VLE Equations

$$Py_i = P_i^0 \gamma_i \phi_i, \qquad i = \text{EG, W}$$
$$\gamma_i = \exp\left[\left(1 - \frac{1}{DP_n}\right)\phi_{\text{poly}} + \chi_i \phi_{\text{poly}}^2\right], \quad i = \text{EG, W}$$

Degree of Polymerization

$$DP_n = 1 + \frac{2x_Z}{(x_{E_g} + x_{E_a})}$$

Real Species Volume Fractions

$$\phi_{\text{EG}} = \frac{\nu_{\text{EG}}\hat{x}_{\text{EG}}}{(\nu_{\text{EG}}\hat{x}_{\text{EG}} + \nu_{\text{W}}\hat{x}_{\text{W}} + \nu_{\text{poly}}\hat{x}_{\text{poly}})}$$
$$\phi_{\text{W}} = \frac{\nu_{\text{W}}\hat{x}_{\text{W}}}{(\nu_{\text{EG}}\hat{x}_{\text{EG}} + \nu_{\text{W}}\hat{x}_{\text{W}} + \nu_{\text{poly}}\hat{x}_{\text{poly}})}$$
$$\phi_{\text{poly}} = 1 - \phi_{\text{EG}} - \phi_{\text{W}} = \frac{\nu_{\text{poly}}\hat{x}_{\text{poly}}}{(\nu_{\text{EG}}\hat{x}_{\text{EG}} + \nu_{\text{W}}\hat{x}_{\text{W}} + \nu_{\text{poly}}\hat{x}_{\text{poly}})}$$

Real Mole Fractions

$$\hat{x}_{\text{EG}} = \frac{x_{\text{EG}}}{[1 - x_Z - (x_{E_g} + x_{E_a})/2]} \qquad \hat{x}_{\text{W}} = \frac{x_{\text{W}}}{[1 - x_Z - (x_{E_g} + x_{E_a})/2]}$$
$$\hat{x}_{\text{poly}} = \frac{[(x_{E_g} + x_{E_a})/2]}{[1 - x_Z - (x_{E_g} + x_{E_a})/2]}$$

Vapor Pressure Correlations

$$\log P_{\text{EG}}^0\ (\text{Pa}) = 11.521 - \frac{3066.5}{T(\text{K})}$$
$$\log P_{\text{W}}^0\ (\text{Pa}) = 10.644 - \frac{2100}{T(\text{K})}$$

Molar Volume Correlations

$$\nu_{\text{EG}}(\text{cm}^3/\text{mol}) = 60.6[1 + 0.0014(T(\text{K}) - 413)]$$
$$\nu_{\text{W}}(\text{cm}^3/\text{mol}) = 19.422 + 0.00138(T(\text{K}) - 413)$$
$$\nu_{\text{poly}}(\text{cm}^3/\text{mol}) \cong 191.5[1 + 0.0014(T(\text{K}) - 413]$$

terms of the apparent mole fractions as

$$K_1 = \frac{x_{E_g} x_{\text{W}}}{2x_{E_a} x_{\text{EG}}} \tag{15a}$$

$$K_2 = \frac{2x_Z x_{\text{W}}}{x_{E_a} x_{E_g}} \tag{15b}$$

$$K_3 = \frac{K_2}{K_1} = \frac{4x_Z x_{\text{EG}}}{x_{E_g}^2}. \tag{15c}$$

The values of these equilibrium constants are listed in Table 5.

Flory–Huggins theory is used to describe the vapor–liquid phase equilibrium. EG and water are considered to be the only volatile components of the reactive mixture. The VLE relationships and thermodynamic parameters are summarized in Table 5. As the system involves solid TPA, we need to consider SLE in addition to VLE to complete our phase equilibrium (VLSE) model.

Reliable models and data on SLE are not available in the open literature. The solubility of solid TPA in EG (c_{EG}) and in polymer (c_{poly}) can be correlated as (Gupta and Kumar, 1987):

$$c_{\text{EG}}(\text{mol TPA/kg solution}) = \exp\left[1.19 - \frac{1{,}240}{T(\text{K})}\right] \tag{16a}$$

$$c_{\text{poly}}(\text{mol TPA/kg solution}) = \exp\left[1.9 - \frac{1{,}420}{T(\text{K})}\right]. \tag{16b}$$

Here we have used the solubility of TPA in BHET for c_{poly}. From the preceding equations, it is evident that TPA is more soluble in the polymer than in EG. From these correlations, with appropriate derivations and change of units, the apparent mole fraction of acid end groups in liquid phase at saturation can be written as

$$x_{E_a}^{\text{sat}} = \frac{\left[2(x_{\text{EG}} + x_{\text{W}}) + x_{E_g}\right](\Sigma s_i \hat{x}_i)}{(1 - \Sigma s_i \hat{x}_i)}, \tag{17}$$

where

$$\Sigma s_i \hat{x}_i = \frac{(0.062\, c_{\text{EG}})}{(1 - 0.166\, c_{\text{EG}})}\hat{x}_{\text{EG}} + \frac{(0.254\, c_{\text{poly}})}{(1 - 0.166\, c_{\text{poly}})}\hat{x}_{\text{poly}}. \tag{18}$$

Although this relation can be used to represent SLE with sufficient accuracy and for obtaining meaningful results from the design approach, experimental studies on the multiphase system of EG–water–TPA–polymer are highly recommended.

Step 2c: Reactive Phase Diagrams. For this example, with E_g and E_a as reference components, the transformed mole fraction coordinates are

$$X_{\text{EG}} = x_{\text{EG}} + \frac{x_{E_g}}{2} - \frac{x_{E_a}}{2} \tag{19a}$$

$$X_{\text{W}} = x_{\text{W}} + x_{E_a} \tag{19b}$$

$$X_Z = 1 - X_{\text{EG}} - X_{\text{W}} = x_z + \frac{x_{E_g}}{2} + \frac{x_{E_a}}{2}. \tag{19c}$$

The reactive phase diagram is as shown in Figures 8a and 8b. The EG–W, E_a–W, and E_a–Z edges are the nonreactive edges. The EG–E_g–Z edge is the reactive edge. EG and water are the only volatile components, and TPA is the only component that can exist in the solid phase. Hence the vapor composition is constrained to lie on the EG–W nonreactive edge and the solid composition always corresponds to vertex E_a.

Figure 8a shows an isothermal reactive phase diagram at 3 atm and 550 K. The shaded triangular region V–L–E_a represents the three-phase region. Within this region, according to the Gibbs phase rule, the system has zero degrees of freedom. Any initial composition within this region would split into vapor, liquid, and solid phases with compositions corre-

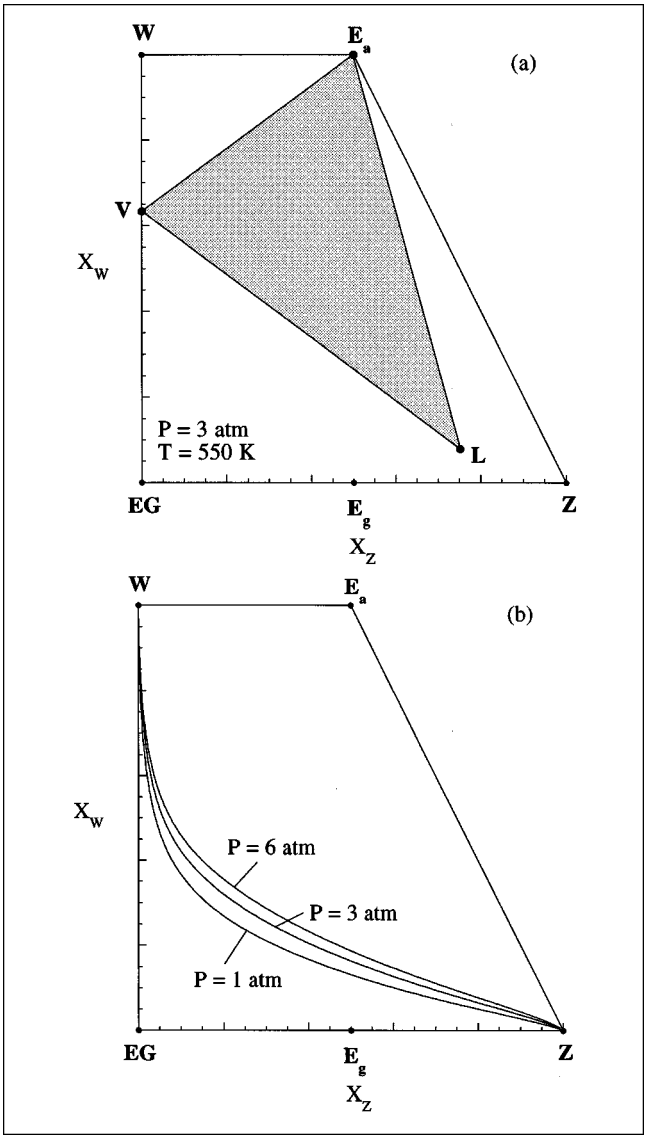

Figure 8. (a) Isothermal reactive phase diagram for Example 2; (b) polythermal reactive phase diagram for Example 2.

In part (a) $P = 3$ atm and $T = 550$ K. The shaded triangular region represents the three-phase region within which solid, liquid, and vapor phases coexist. In part (b) the figure shows solubility curves for $P = 1$, 3, and 6 atm. Temperature varies along the solubility curves.

sponding to points V, L, and E_a, respectively. Outside of this region, the solid phase does not exist and the system has one degree of freedom.

Point L on Figure 8a represents the saturated liquid composition at 3 atm and 550 K. At a given pressure, we can plot the locus of saturated liquid compositions to get a polythermal phase diagram. Figure 8b shows the polythermal reactive phase diagram with saturation curves for pressures of 1, 3, and 6 atm. It can be shown using the arguments presented in the Appendix that when TPA(s) (that is, TPA in solid phase) has completely dissolved, the vapor–liquid reactive system does not show any azeotropes and reactive distillation boundaries.

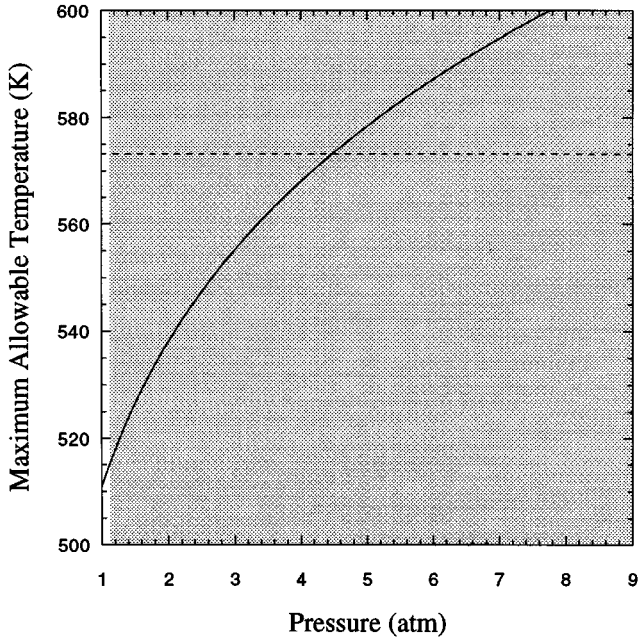

Figure 9. Maximum allowable temperature.

For feasible operation $P \geq 1.1$ atm (shaded area).

Step 3: Feasible Process Flowsheets and Operating Conditions: Pressure and Temperature Range. The $EG-E_g-Z$ reactive edge is a common feature of the reactive phase diagrams of Examples 1 and 2. Phase behavior on this edge is identical for both examples. Hence as for the previous example, at atmospheric pressure, the maximum allowable reaction temperature is 510 K for a degree of polymerization of 2.0 (Figure 4c). However, in this case the reaction temperature should not be less than 513.15 K. Hence operation at atmospheric pressure is not feasible.

The maximum allowable reaction temperature (for $DP_n = 2.0$) increases with increasing pressure, as shown in Figure 9. Note that the maximum allowable temperature is constrained not to exceed 573.15 K (dashed line). The operating pressure has to be within the shaded region ($P > 1.1$ atm) for the maximum allowable temperature to exceed 513.15 K. Depending on the choice of the operating pressure, the reaction temperature is bounded by 513.15 K and the maximum allowable temperature at that pressure. For example, at 3 atm the temperature range is 513.15 K–555.15 K, and at 6 atm it is 513.15 K–573.15 K. It should be noted that in some cases, the choice of operating pressure and corresponding temperature range could be further restricted by the choice of flowsheet configuration. The lightest product of the process is water. It can easily be condensed at pressures greater than 1.1 atm. At high pressures, the condenser can even be used to generate steam.

Feed Ratio. The shape of the phase diagram for this example is identical to that for the previous example. Hence, the feed ratio can be chosen by using exactly the same arguments as before. At all pressures, the ratio of EG to TPA in fresh feed should be in the range 1.23 to 2.33 for $1.5 \leq DP_n \leq 5$. As before, for $DP_n \approx 2$, this ratio should be 1.75. We will use this value in the rest of the discussion.

Feasible Process Flowsheets: CSTR with Separator. This configuration and its reactive phase diagram are shown in Figure 10a. The CSTR operates at a fixed temperature and pressure and acts as a multiphase reactive flash. The vapor, liquid, and solid (if present) phases leaving the reactor are in phase and reaction equilibrium. Complete separation of EG and water in the distillation column is possible as the EG–water mixture does not have any azeotropes at pressures above atmospheric.

The shaded triangular region on the reactive phase diagram corresponds to the three-phase region at the temperature and pressure of reactor operation. Our specifications require us to ensure complete dissolution of solid TPA. The reactive phase diagram shows the limiting case in which at the specified temperature and pressure, solid TPA has just completely dissolved and the prepolymer product corresponds to the saturated liquid composition. Overall material balance indicates that the fresh-feed (stream 3), water (stream 7), prepolymer (stream 5) should lie on a straight line (shown as dashed line). Hence, in the limiting case, fresh-feed composition should correspond to point 3. For feed ratios lower than that for point 3, fresh-feed composition (point 3) would move toward the E_a vertex, and the feed to the reactor (point 4) would move into the triangular three-phase region. Hence, the prepolymer product would contain undissolved TPA. At the given temperature and pressure of operation, the feed ratio corresponding to point 3 is referred to as the critical feed ratio. At the given temperature and pressure, operation of this flow sheet is not feasible below the critical feed ratio.

We have chosen the feed ratio for the process to be 1.75. For the operation to be feasible at this feed ratio, the temperature and pressure of operation should be such that the critical feed ratio at selected temperature and pressure is less than 1.75. Figure 10b shows the minimum allowable temperature for which the critical feed ratio is 1.75 at the given pressure (for $P > 1.1$ atm). The minimum allowable temperature forms the lower bound on the feasible reaction temperature; the upper bound (given by Figure 9) is also shown in Figure 10b. At low pressures (near 1.1 atm), the range of the feasible temperature is very narrow. Hence, a pressure of 5 atm for which the operating temperature range is sufficiently broad (533.45 K–573.15 K) is chosen.

For this configuration, the conversion is low at lower temperatures, and the amount of EG in the recycle stream is very high at higher temperatures. Hence, while it provides a good starting point to understand the system, it is not very useful from a practical standpoint.

Cascade of CSTRs with Separator. Here again, the preceding problem can be solved by using a cascade of CSTRs with a stepwise increase in operating temperature. Figure 11 shows a flowsheet and reactive phase diagram for this configuration. Complete dissolution of TPA in the first reactor is ensured by using the pressure and temperature ranges determined earlier.

Typically, three reactors in series, as shown in Figure 11, are adequate. The first reactor is operated at the lowest allowable temperature 535.4 K, the last reactor is operated at the highest possible temperature 573.15 K, and the middle reactor is operated at an intermediate temperature of 554.28 K. This cascade of reactors gives the same conversion as a single CSTR operating at 573.15 K, but the ratio of EG in the recycle stream to the EG in the fresh feed is only 3.19, a significant reduction from 10.2.

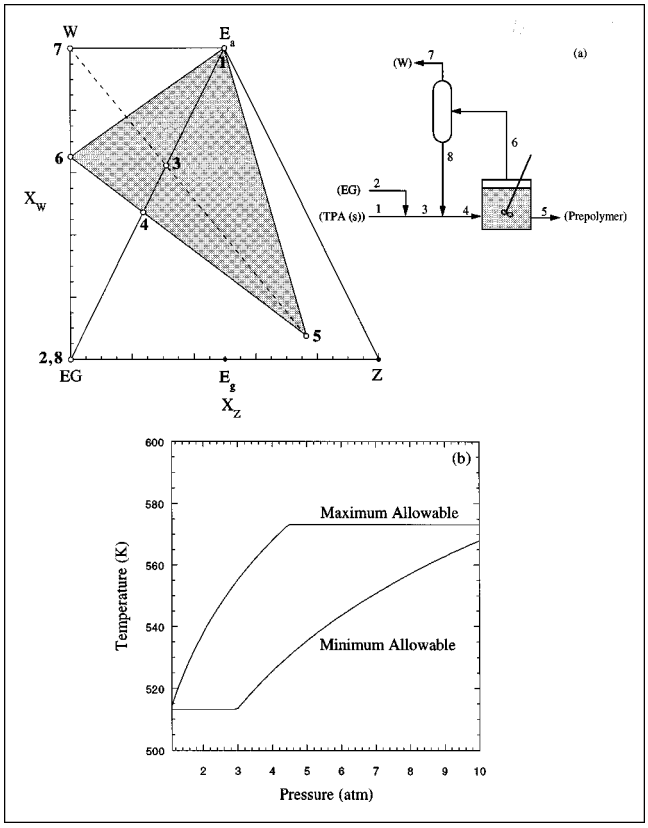

Figure 10. (a) Flowsheet and reactive phase diagram for CSTR with separator; (b) temperature range for feasible operation.

In part (a) the reactive phase diagram depicts the limiting case at which TPA(s) has just completely dissolved in the liquid phase at the given T and P. Minimum allowable temperature shown in part (b) ensures complete dissolution of TPA(s) and maximum allowable temperature ensures $DP_n \leq 2.0$.

As pointed out before, the cascade of CSTRs is equivalent to a PFR. However, the cascade is not replaced by a PFR for this example, as maintaining an increasing temperature profile and vapor removal along the entire length of the PFR, and handling TPA(s) without settling, fouling, and so on, is extremely difficult.

Flowsheet Configurations Involving Reactive Distillation: Reactive Distillation Column Fed Through Reboiler. Top product compositions on the EG–W edge and bottoms compositions anywhere on the reactive phase diagram can be obtained using a reactive distillation column, as the reacting system does not show any azeotropes and reactive distillation boundaries (see the Appendix). However, the TPA feed to the process is in solid state. We wish to avoid handling solids in a distillation column to prevent fouling and related operational difficulties. Hence, TPA(s) cannot be fed to the distillation column unless it is completely dissolved in the reaction mixture. In addition, T and P on each tray of the column should not allow precipitation of TPA. We can try to dissolve TPA(s) into the reaction mixture before it is fed to the column by using a CSTR before the column, as shown in Figure

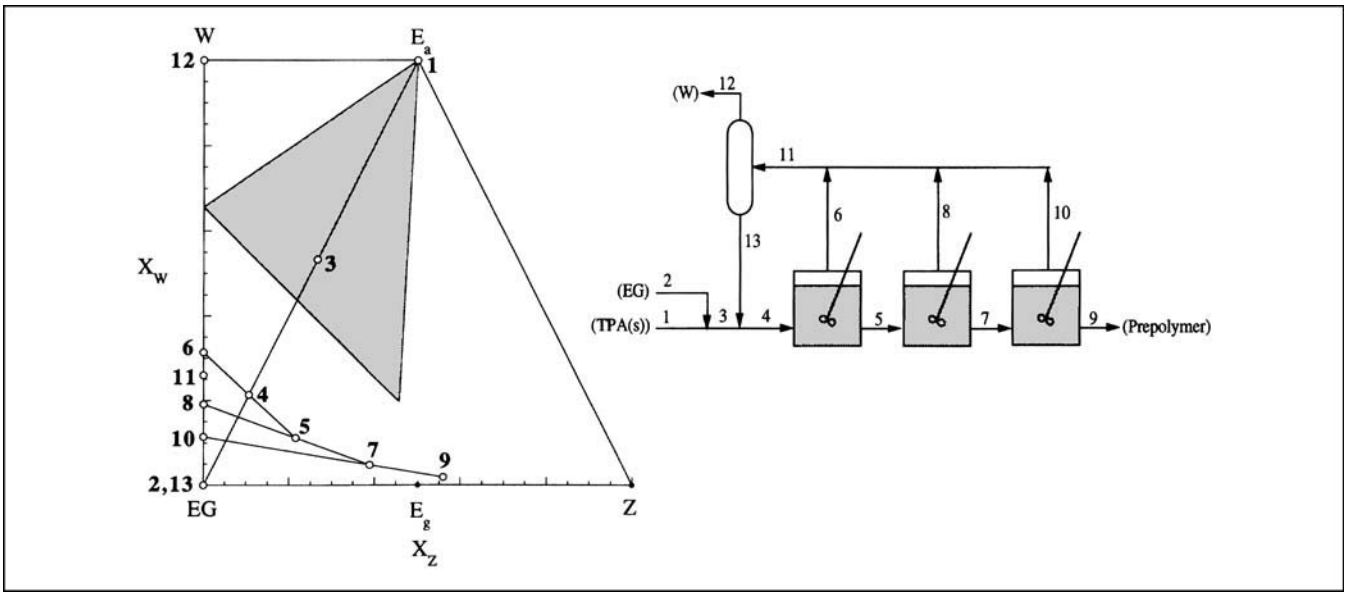

Figure 11. Flowsheet and reactive phase diagram for cascade of CSTRs with separator: $T_1 = 535.4$ K, $T_2 = 554.28$ K, $T_3 = 573.15$ K, $P = 5$ atm.

12a. This reactor acts as the reboiler for the distillation column, and the resulting configuration is a modification of the reactive distillation configuration of Figure 3d. TPA(s) and EG are fed to the reboiler. The liquid and vapor streams from the reboiler form the feed to the distillation column. Water (condensate) is removed from the top and the prepolymer product is removed from the bottom tray.

Figure 12a also shows the reactive phase diagram for this process. For feasible operation, the liquid stream from the reboiler (stream 4) should not contain any undissolved TPA. The reactive phase diagram depicts the limiting case in which at specified T and P, TPA(s) has just completely dissolved and stream 4 corresponds to the saturated liquid composition. For this limiting case, the feed ratio corresponds to point 3 (critical feed ratio). At the specified T and P, complete dissolution of TPA is not possible for feed ratios less than this critical value. Figure 12b shows the critical feed ratio as a function of temperature for pressures of 1.1, 2.1, 5 and 6 atm. We have chosen the feed ratio for the process to be 1.75. The critical feed ratio is always higher than 1.75 in this P and T range. Hence, for an EG to TPA(s) ratio of 1.75 in the feed, TPA will never dissolve completely in the reboiler at any given T and P, and the configuration is infeasible. We must make some modifications to this configuration in order to use the reactive distillation column.

Reactive Distillation Columns with Recycle Streams. The following modifications involve changing the stream destinations in the configuration of Figure 12a to make it feasible in the desired range of operating temperature and pressure.

Reactive Distillation Column with Product Recycle. If we compare the flowsheets and phase diagrams of Figures 10a and 12a, we can see that the CSTR in Figure 10a has a recycle stream (stream 8) that provides the additional EG to completely dissolve TPA(s). Hence, we can make the process in Figure 12a feasible if we can provide the reboiler with a recycle stream that can ensure complete dissolution of TPA(s).

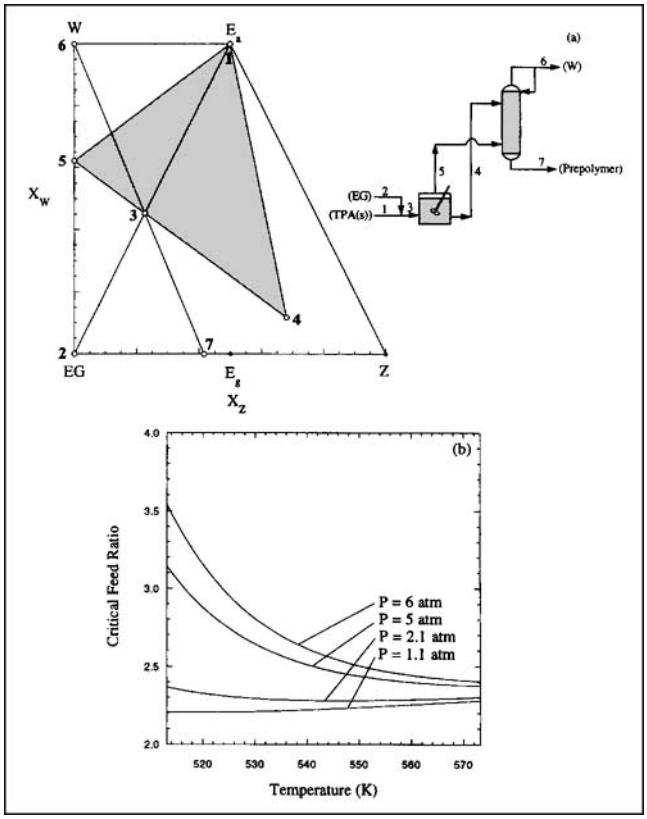

Figure 12. (a) Flowsheet and reactive phase diagram for reactive distillation column fed through reboiler; (b) critical feed ratios at $P = 1.1$, 2.1, 5 and 6 atm.

In part (a) the reactive phase diagram depicts the limiting case at which TPA(s) has just completely dissolved in the reboiler at the specified T and P. As shown in part (b), operation at EG to TPA feed ratio of 1.75 is infeasible at all pressures.

The simplest modification that can be done is to recycle a part of the prepolymer product. The flowsheet and corresponding reactive phase diagram are shown in Figure 13a. The recyle stream brings the feed out of the three-phase region (shaded triangular region) at the expense of increased reboiler size and duty. The column and the reboiler both operate at 5 atm. The reboiler is operated at the maximum allowable temperature of 573.15 K. The temperature at the top of the column is 425.15 K (bubble point of condensate at 5 atm), and the prepolymer product is removed from the last tray at 573.15 K. The temperature below the tray at which the liquid stream (stream 5) is fed is greater than 535.4 K (minimum allowable temperature).

It should be noted that a similar recycle stream could also be included in flowsheets of Figures 10a (CSTR) and 11 (cascade of CSTRs). In these cases, the recycle stream does not change the operating temperature range shown in Figure 10b. However, it reduces the amount of EG in the recycle stream, thereby reducing the separation cost at the expense of increased reactor and recycle cost.

Reactive Distillation Column Fed Through Intermediate Reboiler. EG recycle can also be provided by using an intermediate reboiler to feed the reactive distillation column, as shown in Figure 13b. EG and TPA(s) (feed ratio of 1.75) are fed to the intermediate reboiler. The vapor and liquid streams leaving the reboiler form the feed streams to the reactive section (shaded portion) of the reactive distillation column. The reactions take place in this zone, which also aids in separating EG from water. The nonreactive section of the column does not contain any polymeric species and essentially performs the task of separating EG from water. The liquid stream from the last tray of the nonreactive section, which is essentially EG, is sent to the the intermediate reboiler. This stream provides the additional EG necessary to ensure complete dissolution of TPA(s) in the reboiler (as can be seen from the reactive phase diagram in Figure 13b). The vapor stream leaving the top of the reactive section (shown by an unnamed arrow) forms the feed to the nonreactive section. The prepolymer product is taken out from the bottom tray of the reactive section and the condensate is removed from the top of the nonreactive section.

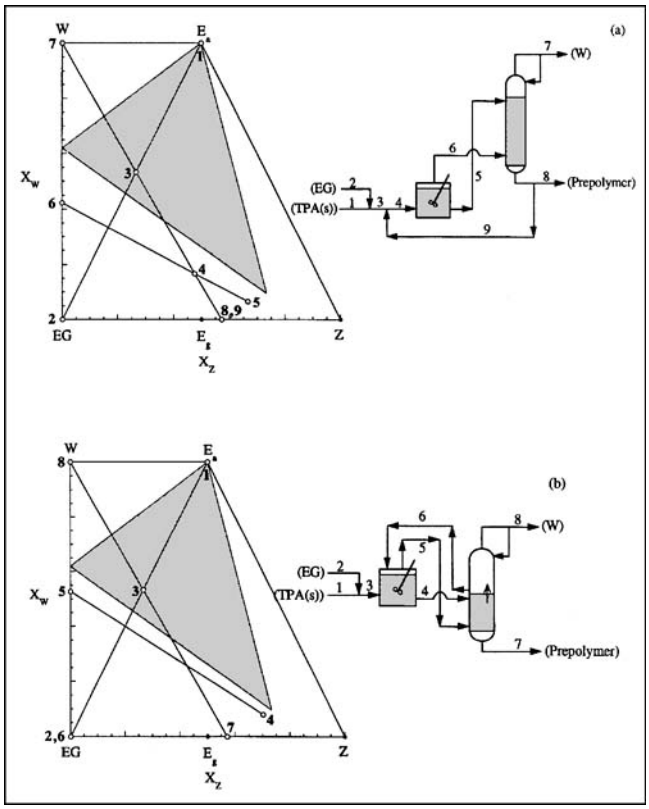

Figure 13. Flowsheet and reactive phase diagram for: (a) reactive distillation column with product recycle; (b) reactive distillation column fed through intermediate reboiler.

The process is operated at 5-atm pressure. The reboiler is operated at 573.15 K. The prepolymer is removed at the same temperature. The temperature at the top of the nonreactive section is 425.15 K, while the temperature at the boundary between the reactive and nonreactive section is 535.4 K. Exchange of heat between streams 4 and 6 can be done for heat integration.

Reactive Distillation Columns with Distributed Addition of TPA(s). These configurations are arrived at by adding additional units or combining configurations. Complete dissolution of TPA(s) at operating T and P is ensured by using the distributed addition of TPA(s). Figure 14a shows a flow sheet comprising a reactive distillation column with two reboilers. The process is operated at 5 atm. Both the reboilers are operated at 573.15 K. The reactive distillation column is fed through the first reboiler. Only a part of the TPA(s) is fed to this reboiler along with EG so that the feed ratio is greater than the critical value of 2.38. The vapor and liquid streams form the feed to the reactive distillation column. The second reboiler acts as a conventional reboiler for the column. The remaining part of the TPA feed is added to the bottoms product of the reactive distillation column before sending it to this reboiler. The liquid stream from this reboiler is the prepolymer product, and the vapor stream is sent back to the column. The condensate is removed at the top at a temperature of 425.15 K.

Figure 14b shows a flow sheet comprising two reactive distillation columns fed through two reboilers. The process is operated at 5 atm pressure with both reboilers operating at 573.15 K. The feed to the first reboiler is the EG and TPA(s) in a ratio of 3:1. The vapor and liquid streams from this reboiler form the feeds to the first column. The liquid product from the bottom tray of the first column is mixed with the remaining TPA(s) to form the feed to the second reboiler, which feeds the second column. The prepolymer product is taken out from the bottom tray of the second column at 573.15 K. The condensate is removed from the top of both columns at 425.15 K. The phase diagram for this configuration is shown in Figure 14c. It can be seen clearly that incomplete dissolution is avoided by distributing TPA(s) over two reboilers (streams 3 and 9 lie outside the shaded three-phase region). This configuration may be unattractive, as it uses two reactors and two columns, although significantly smaller columns are required for reactive distillation.

Residence Time. For the CSTR cascade of Figure 11, the average residence times for the first, second, and third reac-

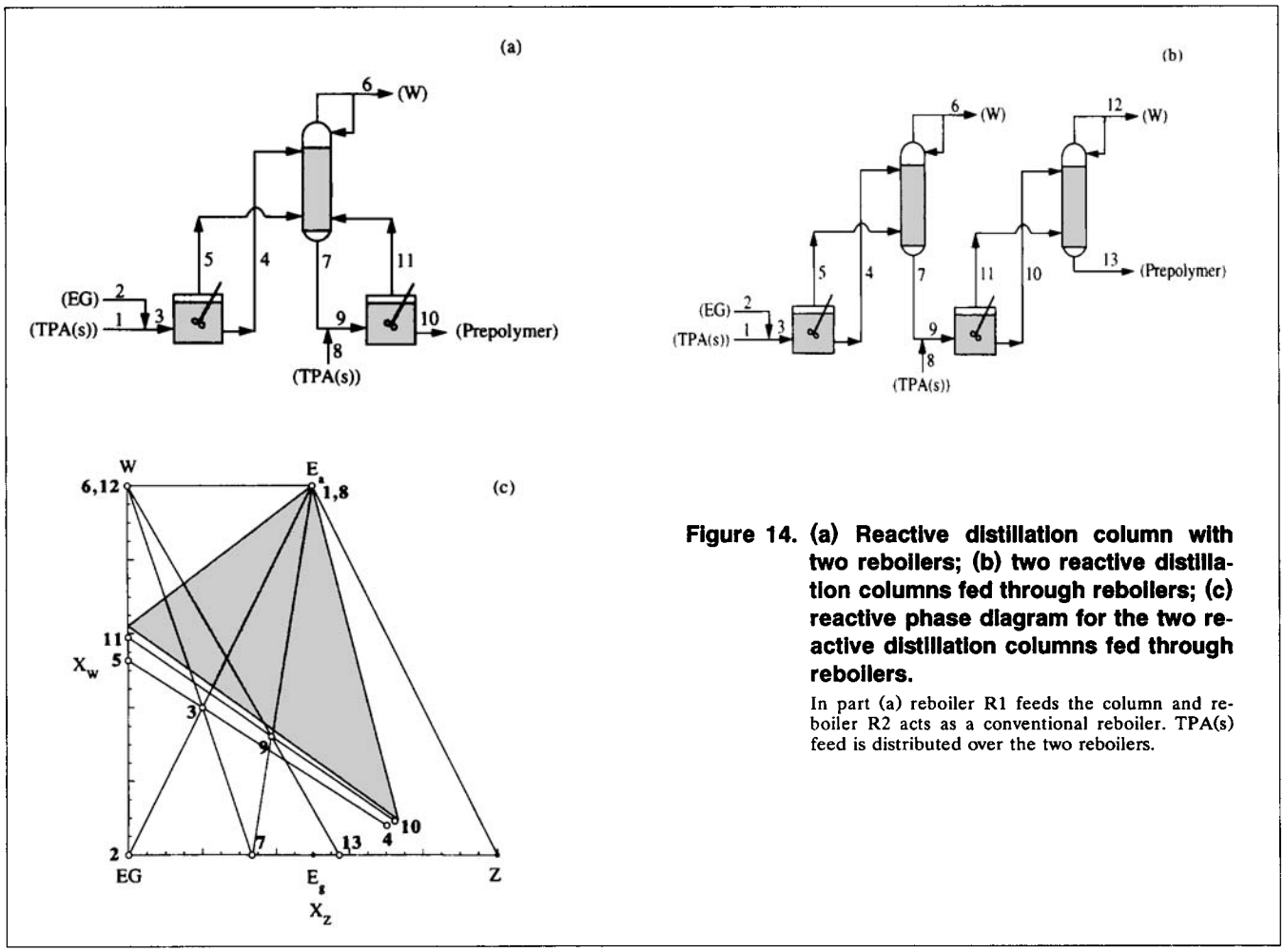

Figure 14. (a) Reactive distillation column with two reboilers; (b) two reactive distillation columns fed through reboilers; (c) reactive phase diagram for the two reactive distillation columns fed through reboilers.

In part (a) reboiler R1 feeds the column and reboiler R2 acts as a conventional reboiler. TPA(s) feed is distributed over the two reboilers.

tors should be much greater than 4.61 min, 2.55 min, and 1.47 min, respectively. In estimating these lower bounds, dissolution of TPA(s) is not considered as a rate-limiting factor, as it is found to be instantaneous over a range of particle sizes (Kemkes, 1969).

Summary and Comparison with Simulation. Table 6 presents a summary of the feasible process alternatives developed for this example and the corresponding operating conditions. Literature references to some of the configurations are also listed. The table also presents a comparison of operating conditions determined by using repeated simulations of a cascade of CSTRs with separator (Ravindranath and Mashelkar, 1982c) and our design approach. The operating conditions determined by our approach are in good agreement with those determined through simulations. However, it should be noted that we could develop these operating conditions only on the basis of equilibrium phase behavior without performing extensive simulations. In addition, the design approach also led us to many other feasible flowsheets. To assess the accuracy of the design approach, a comparison with simulations is also presented in Table 6 for a cascade of CSTRs with separator operating at the conditions developed earlier.

Example 3: production of Nylon-6,6

Nylon-6,6 is produced from HMDA and AA monomers. Like PET, nylon-6,6 production uses all three stages of polycondensation shown in Figure 1. However, the prepolymerization stage for Nylon-6,6 is not as widely studied as the polymerization (Kumar et al., 1981, 1982), and the finishing stages (Choi and Lee, 1996; Guidici et al., 1997; Steppan, 1989).

Step 1: Specifications. Nylon-6,6 can be prepared starting directly from molten monomers or starting from nylon salt (hexamethylene diammonium adipate) that is prepared from the monomers. Nylon salt is easier to transport and store than the monomers. However, direct use of molten monomers is preferred, as most production plants manufacture the monomers at the same site. In this example, we will consider the molten monomers, HMDA and AA, as starting raw materials. The specifications for this example are:

- Input specifications
  Raw materials are molten HMDA and AA.
- Output specifications
  Relative viscosity (defined below) of prepolymer product should not exceed 3 to 5.

Table 6. Summary of Results for Example 2

Feasible Process Alternatives

1. Cascade of CSTRs with separator (Gupta and Kumar, 1987; Ravindranath and Mashelkar, 1986a)
2. Reactive distillation column with product recycle
3. Reactive distillation column fed through intermediate reboiler
4. Reactive distillation column(s) with distributed addition of TPA(s)

*Feasible Operating Conditions and Comparison with Results of Repeated Simulations**

Oper. Condition	Our Approach	Repeated Simul.
Feed ratio (EG/DMT)	1.75	1.3 to 1.9
Pressure	$P \geq 1.1$ atm ($P = 5$ atm is used)	3 to 6 atm
Temperature range	535.4 to 573.15 K (for $P = 5$ atm)	513.15 to 553.15 K
Residence time (for a 3 CSTR cascade)	$\tau_1 > 4.61$ min $\tau_2 > 2.55$ min $\tau_3 > 1.47$ min	$\tau_1 = 90$ min $\tau_2 = 60$ min $\tau_3 = 30$ min

Comparison with Simulation for a Cascade of Three CSTRs with Separator

Specification	Desired	For Oper. Cond. Determined Above
DP_n of prepolymer product	2.0	1.9638
x_{E_a} in prepolymer product	0.0	8.553×10^{-3}
x_W in prepolymer product	0.0	1.093×10^{-2}
Undissolved TPA in prepolymer product	None	None
Reactor temperature	< 573.15 K	535.4 K to 573.15 K (for $P = 5$ atm)

*Ravindranath and Mashelkar (1982c).

Table 7. Reaction Kinetics for Example 3

Representation of Kinetic Scheme

1. $E_a + HMDA \leftrightarrow E_n + W$
2. $E_a + E_n \leftrightarrow Z + W$

HMDA: Hexamethylene diamine ($H_2N-(CH_2)_6-NH_2$)
W: Water (H_2O)
Z: Polymer linkage (---CONH---)
E_a: Carboxylic acid end group (---COOH)
E_n: Amine end group (---CONH-$(CH_2)_6$-NH_2)

(N.B.: Both reactions represent the same chain buildup mechanism. However, HMDA is treated as separate from amine end groups, as it is volatile and has to be incorporated in the phase equilibrium model).

Rate Expressions

1. $R_1 = k\left(x_{E_a}x_{HMDA} - \frac{x_{E_n}x_W}{K}\right)$
2. $R_2 = k\left(x_{E_a}x_{E_n} - \frac{x_Z x_W}{K}\right)$

*Kinetic Parameters**

$$k(1/h) = k_0 \exp\left[\frac{-E}{R}\left(\frac{1}{T(K)} - \frac{1}{473.15(K)}\right)\right]$$

$$k_0(1/h) = \exp\{2.55 - 0.45\tanh[25(x_W - 0.55)]\} + 8.58\{\tanh[50(x_W - 0.10)] - 1\}(1 - 30.05x_{E_a})$$

$$E = 21{,}400 \text{ cal/mol}$$

*Steppan (1989).

Negligible loss of volatile monomer (HMDA).

Complete conversion of HMDA.

The ratio of mole fractions of acid end groups and amine end groups should be close to unity.

- Constraints

Maximum operating temperature should be in the range of 543.15 K to 573.15 K.

The relative viscosity of the polymer is typically used as a measure of degree of polymerization. It is defined as the ratio of viscosity (in centipoise) at 298.15 K of 8.4% by weight solution of the nylon polymer in 90% formic acid (90% by weight formic acid, 10% by weight water) to the viscosity (in centipoise) at 298.15 K of 90% formic acid alone (Jaswal and Pugi, 1975). The relative viscosity can be related to the degree of polymerization as

$$\log(\bar{\eta}) = 1.4\log(113DP_n) - 4.2021. \qquad (20)$$

This equation is derived from the information obtained from Jacobs and Zimmerman (1977) on relative viscosities of nylon polymers of different average molecular weights. From this equation the viscosity limit translates to a degree of polymerization of 19.46 to 28.03. Hence, DP_n of the prepolymer product should be less than 25. The loss of valuable volatile monomer HMDA should be negligible to prevent disruption of end-group stoichiometry and to eliminate the environmental pollution problems occasioned by the release of HMDA to the atmosphere. In addition, it is necessary to ensure almost complete conversion of HMDA to make sure that the loss of HMDA in subsequent polymerization and finishing stages is minimal. The reason we want to maintain the ratio of mole fractions of acid and amine end groups close to unity will become clear when we consider the kinetic scheme. The temperature constraint is imposed to limit various thermal degradation reactions that take place at elevated temperatures (Steppan, 1989).

Step 2a: Representation of Kinetic Scheme. The major reactions involved can be written in terms of functional end groups, as shown in Table 7. The rate expressions and kinetic parameters are also listed in Table 7. The expressions for rate constants were developed by Steppan (1989) by correlating experimental data from several investigators. The rate constants are found to be functions of temperature and mole fractions of water and acid end groups. It can be seen from Table 7 that the chain buildup in both reactions takes place through the same mechanism. This is in contrast to the previous examples, where we had two chain buildup mechanisms. Both reactions involve an acid end group and an amine end group (either on HMDA as in reaction 1 or on a polymer chain as in reaction 2). Hence, the prepolymer product needs to have the acid and amine end groups in a 1:1 stoichiometric ratio to ensure further chain buildup to an appreciable DP_n in the polymerization and finishing stages. This is the reason we wanted to maintain the ratio of mole fractions of acid and amine end groups close to unity.

In addition to the reactions just cited, many possible degradation reactions are postulated in the literature. We do not include these in our analysis, however, as sufficient information on their mechanisms and kinetic parameters is not available. To limit the production of side products, we limit the operating temperature to 543.15 K to 573.15 K as suggested by Steppan (1989).

Table 8. Thermodynamic Parameters for Example 3

*Reaction Equilibrium Constant**

$$K = K_0 \exp\left[\frac{-\Delta H}{R}\left(\frac{1}{T(\mathrm{K})} - \frac{1}{473.15(\mathrm{K})}\right)\right]$$

$$K_0 = \exp\left\{\left[1 - 0.47\exp\left(\frac{x_W^{0.5}}{0.2}\right)\right](8.45 - 4.2x_W)\right\}$$

$$\Delta H(\mathrm{cal/mol}) = 7{,}650\tanh[6.5(x_W - 0.52)] + 6{,}500\exp\left(\frac{-x_W}{0.065}\right) - 800$$

VLE Equations

$$Py_i = P_i^0\gamma_i\phi_i, \qquad i = \mathrm{HMDA, W}$$

$$\gamma_i = \exp\left[\left(1 - \frac{1}{DP_n}\right)\phi_{poly} + \chi_i\phi_{poly}^2\right], \quad i = \mathrm{HMDA, W}$$

Degree of Polymerization

$$DP_n = 1 + \frac{2x_Z}{(x_{E_n} + x_{E_a})}$$

Real Species Volume Fractions

$$\phi_{HMDA} = \frac{\nu_{HMDA}\hat{x}_{HMDA}}{(\nu_{HMDA}\hat{x}_{HMDA} + \nu_W\hat{x}_W + \nu_{poly}\hat{x}_{poly})}$$

$$\phi_W = \frac{\nu_W\hat{x}_W}{(\nu_{HMDA}\hat{x}_{HMDA} + \nu_W\hat{x}_W + \nu_{poly}\hat{x}_{poly})}$$

$$\phi_{poly} = 1 - \phi_{HMDA} - \phi_W = \frac{\nu_{poly}\hat{x}_{poly}}{(\nu_{HMDA}\hat{x}_{HMDA} + \nu_W\hat{x}_W + \nu_{poly}\hat{x}_{poly})}$$

Real Mole Fractions

$$\hat{x}_{HMDA} = \frac{x_{HMDA}}{[1 - x_Z - (x_{E_n} + x_{E_a})/2]}$$

$$\hat{x}_W = \frac{x_W}{[1 - x_Z - (x_{E_n} + x_{E_a})/2]}$$

$$\hat{x}_{poly} = \frac{[(x_{E_n} + x_{E_a})/2]}{[1 - x_Z - (x_{E_n} + x_{E_a})/2]}$$

Vapor Pressure Correlations

$$\log P_{HMDA}^0\ (\mathrm{Pa}) = 11.7206 - \frac{3{,}054.7}{T(\mathrm{K})}$$

$$\log P_W^0\ (\mathrm{Pa}) = 10.664 - \frac{2{,}100}{T(\mathrm{K})}$$

Molar Volume Correlations

$$\nu_{HMDA}(\mathrm{cm^3/mol}) = 136.70 + 0.00138\,(T(\mathrm{K}) - 413)$$
$$\nu_W(\mathrm{cm^3/mol}) = 19.422 + 0.00138\,(T(\mathrm{K}) - 413)$$
$$\nu_{poly}(\mathrm{cm^3/mol}) \cong 136.70 + 0.00138\,(T(\mathrm{K}) - 413)$$

*Steppan (1989).

Step 2b: Phase and Reaction Equilibria. The correlations by Steppan (1989) for the equilibrium constant are listed in Table 8. The equilibrium constant is found to be a function of temperature and the mole fraction of water in the reaction mixture.

For the reactive system comprising HMDA, AA, water, and polymer, very limited information on thermodynamic behavior is available. Here, we use Flory-Huggins theory to describe the vapor–liquid phase equilibrium, as was done for the previous examples. HMDA and water are considered to be the only volatile components of the reaction mixture. The VLE relationships and thermodynamic parameters are also summarized in Table 8. Experimental studies on the reactive system are highly recommended, and experimental data, if available, can be substituted for our VLE model.

Step 2c: Reactive Phase Diagrams. The reactive system comprises five apparent components and two reactions. Hence, we have three transformed mole fractions, of which two are independent. With E_n and E_a as reference components, the transformed mole fraction coordinates are

$$X_{HMDA} = x_{HMDA} + \frac{x_{E_n}}{2} - \frac{x_{E_a}}{2} \tag{21a}$$

$$X_W = x_W + x_{E_a} \tag{21b}$$

$$X_Z = 1 - X_{HMDA} - X_W = x_z + \frac{x_{E_n}}{2} + \frac{x_{E_a}}{2}. \tag{12c}$$

The shape of the reactive phase diagram in terms of the independent transformed coordinates X_Z and X_{HMDA} is as shown in Figure 15. The HMDA–W, E_a–W, and E_a–Z edges are the nonreactive edges, and the HMDA–E_n–Z edge is the reactive edge. Any composition within the phase diagram corresponds to an equilibrium mixture of all five apparent components. The vapor composition is constrained to lie on the HMDA–W nonreactive edge, while liquid composition can lie anywhere on the phase diagram. The binary system of HMDA and water is decidedly nonideal, but does not possess any azeotropes. Hence using the arguments presented in the Appendix, we expect the reactive systems to be free of azeotropes and reactive distillation boundaries.

Step 3: Feasible Process Flowsheets and Operating Conditions: Feed Ratio. As noted earlier, unlike the previous two examples, this example possesses only one chain buildup mechanism that involves acid and amine end groups. The acid end groups in the feed are in the form of AA and the amine end groups are in the form of HMDA. AA is not considered volatile and hence acid end groups are not lost through the process. Also, if all HMDA fed to the process is converted and none is lost through the process, then it should appear in

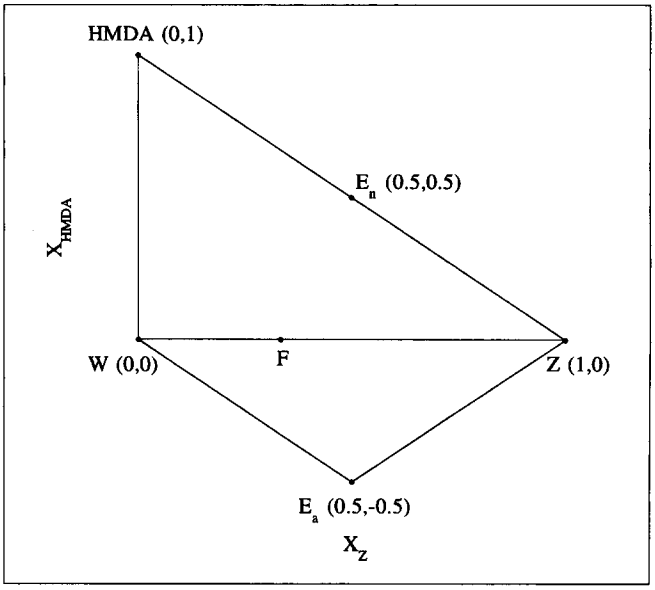

Figure 15. Shape of the reactive phase diagram for Example 3.

the prepolymer product as amine end groups on polymer chains. Thus for a 1:1 ratio of acid and amine end groups in the final product, this ratio should be 1:1 in the feed to the process. Hence, we will use an HMDA to AA ratio of unity in the feed, and ensure maximum conversion and minimum loss of HMDA through proper choice of other operating conditions.

Pressure and Temperature Range. The overhead product for this example is water. Hence, it can easily be condensed at or above atmospheric pressure. As for the previous example, however, in this case the pressure range is governed by the desire to obtain reasonable reaction rates, as demonstrated below.

For the HMDA to AA ratio of unity, the feed composition corresponds to point F on the reactive phase diagram of Figure 15. The overall material balance on the prepolymer stage indicates that the feed, prepolymer product, and condensate (water) should lie on a straight line. Thus, depending on the temperature and pressure of operation, the prepolymer composition would lie on the $F-Z$ portion of line W$-Z$. Every point on $F-Z$ has $5(c)-2(r)-2(p)+2-2(X_Z$ and X_{HMDA} are specified$)=1(f)$ degree of freedom. Hence, at the given pressure, every point on $F-Z$ has a unique temperature associated with it. Figure 16a shows the temperature (corresponding to point F) and the lower bound on the average reactor residence time as a function of pressure. The lower bound on average residence time is estimated as

$$\tau_{\min} = \frac{1}{k}, \tag{22}$$

where the forward reaction rate constant is calculated using the correlations of Table 7. The reactor residence time should be much greater than the lower bound for the system to be at reaction equilibrium and for our design results to be accurate. For a reasonable lower bound on the residence time ($\tau_{\min} \leq 30$ min), the pressure has to be greater than 8 atm (shaded area on Figure 16a). $P = 16$ atm for which $\tau_{\min} = 6$ min is chosen.

Figure 16b shows the temperature and degree of polymerization at different points on $F-Z$ at $P = 16$ atm. For $DP_n \leq 25$, the operating temperature should be greater than 474.65 K (shaded area). The temperature corresponding to point F (475.35 K) provides the upper bound on the temperature range at 16 atm. This range is very narrow. Thus we can use $T = 475.15$ K, for which $DP_n = 15$. Note that this operating temperature does not violate the temperature constraint.

Residence Time. For operation at 16 atm and 475.15 K, the average residence time should be much greater than 6 min.

Feasible Process Flowsheets: CSTR with Separator. The flowsheet for this configuration is shown in Figure 17a. The reactor is operated at 16 atm and 475.15 K. HMDA is separated from water in the vapor stream in the separator and recycled back to the reactor. It is not necessary to use a cascade of CSTRs for this process, as product specifications can be easily attained using one CSTR.

Reactive Distillation Column. As before, the number of stages required for separation of HMDA and water can be significantly reduced by making HMDA react with AA in the

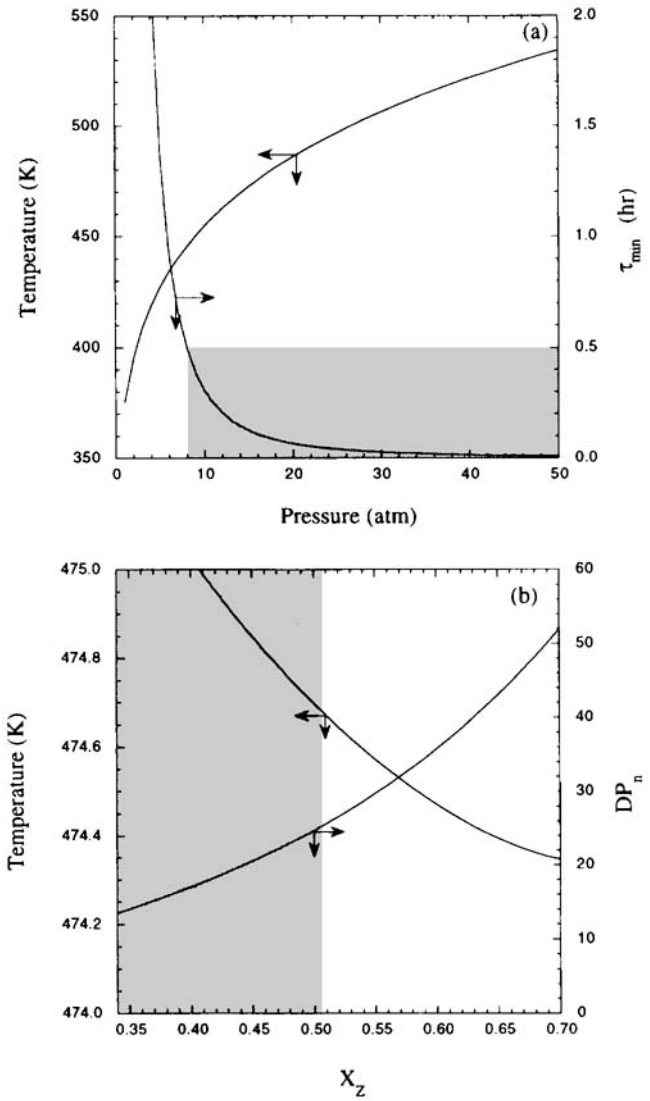

Figure 16. (a) Temperature and lower bound on residence time as functions of operating pressure; (b) temperature and degree of polymerization as functions of prepolymer product composition at 16 atm.

distillation column. Such a reactive distillation column is shown in Figure 17b. HMDA is added near the bottom of the column and AA is fed near the top. AA reacts with HMDA as it travels down the column, thus aiding its separation from water. The column is operated at 16 atm. The temperature at the bottom of the column is 475.15 K, and at the top it is around 465 K.

Reactive Distillation Column Fed Through Reboiler. In the reactive distillation column shown in Figure 17b, reaction occurs near the top of the column at temperatures lower than 475.15 K. This can be rectified by feeding the reactor through a reboiler as discussed for Example 1. The flow sheet and reactive phase diagram for such a configuration is shown in Figure 17c. The reboiler operates at 16 atm and 475.15 K. The vapor stream from the reboiler is fed near the bottom of the reactive distillation column and the liquid stream is fed

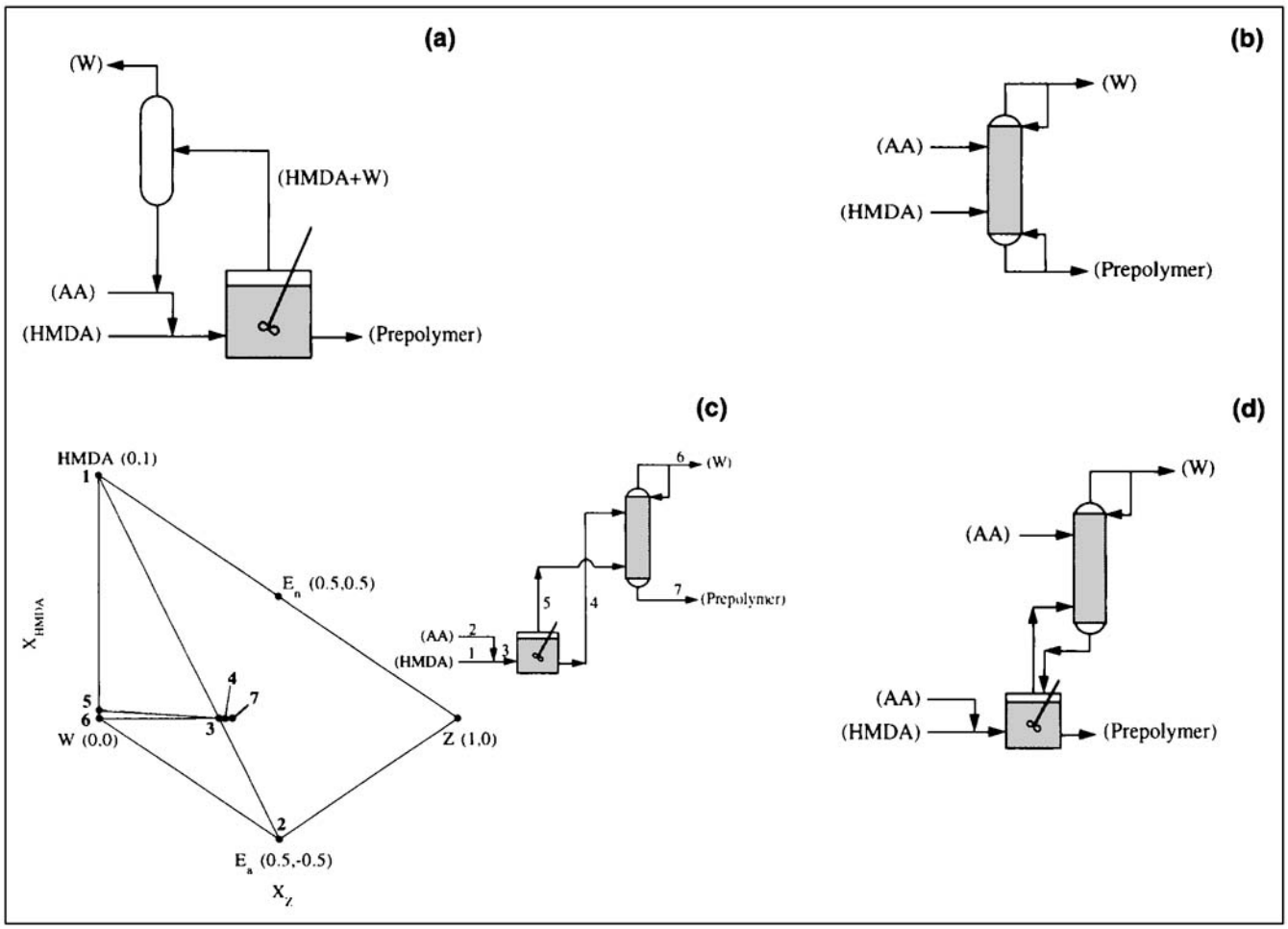

Figure 17. (a) CSTR with separator for Example 3; (b) reactive distillation column for Example 3; (c) flow sheet and reactive phase diagram for reactive distillation column fed through reboiler; (d) combination of configurations of Figures 17b and 17c.

near the top. The prepolymer product is removed from the bottom tray of the column.

Figure 17d shows a combination of configurations of Figures 17b and 17c. In this configuration the reboiler, which operates at 18 atm and 475.15 K, is fed with HMDA and a part of AA. The reboiler supplies the vapor feed to the distillation column, and the liquid feed is provided by the remaining AA. The product is removed from the reboiler instead of the last tray of the column. A summary of results for this example and comparison of operating conditions with literature values is presented in Table 9.

Conclusions

In the prepolymerization stage of a polycondensation process, a short-chain prepolymer suitable for further reaction in the polymerization and finishing stages is prepared. Its main function is to ensure that operational limitations due to stoichiometry, thermodynamics, and so on, do not propagate onto the subsequent stages. Proper design of the prepolymerization stage is critical for the successful operation of the entire polycondensation process.

Earlier approaches have all been based on design through performance simulations. While simulations allow tuning of the design variables (operating conditions) for a specified flow sheet, to meet the desired design specifications, they provide

Table 9. Summary of Results for Example 3

Feasible Process Alternatives		
1. CSTR with separator (Jaswal and Pugi, 1975)		
2. Reactive distillation column		
3. Reactive distillation column fed through reboiler		
4. Combination of 2 and 3 (Sauerbrunn, 1983)		
*Feasible Operating Conditions and Comparison with Literature Values**		
Oper. Condition	Our Approach	Jaswal and Pugi
Feed ratio (HMDA/AA)	1.0	1.0
Pressure	$P \geq 8$ atm ($p = 16$ atm is used)	10 to 24 atm
Temperature range	475.15 K (for $P = 16$ atm)	488.15 K to 518.15 K
Avg. residence time	> 6 min	40 min to 200 min

*Jaswal and Pugi (1975).

little insight for generating alternative flowsheet configurations. To fill this gap, a design method based on an analysis of equilibrium-phase behavior of reactive systems has been developed.

Models in terms of real and apparent mole fractions are used to describe phase and reaction equilibria in polycondensation systems. Transformed mole fractions are used to visualize the reactive phase diagrams from which insights are obtained for developing feasible process alternatives and operating conditions. The procedure is illustrated with three examples, each with its unique features. The operating conditions obtained from the analysis of reactive phase behavior are in excellent agreement with those obtained from simulations and those used in industrial practice. In addition, many flowsheet alternatives that can meet the desired process specifications are identified. The procedure is sufficiently general, and with proper considerations can easily be applied to other polycondensation systems. Efforts are underway to extend our method to the finishing stage of the polycondensation process, which unlike the prepolymerization stage is severely limited by mass transfer.

Acknowledgment

Financial support from the National Science Foundation (Grant No. 9807101) is gratefully acknowledged.

Notation

A_i = frequency factor of the forward reaction rate of reaction i, 1/min
E_i = activation energy of the forward reaction rate of reaction i, kcal/mol
K_i = thermodynamic equilibrium constant of reaction i
N_T = total number of moles of apparent components
$\hat{N}_T$ = total number of moles of real components
P = pressure, atm
P_i^0 = vapor pressure of volatile component i, atm
R = universal gas constant, $R = 1.987$ cal/(mol)(K)
T = temperature, K
x_i = mole fraction of apparent component i in liquid phase
y_i = mole fraction of volatile component i in vapor phase
Z = polymer linkage
ϕ_i = volume fraction of real component i in liquid phase

Literature Cited

Berry, D. A., and K. M. Ng, "Synthesis of Reactive Crystallization Processes," *AIChE J.*, **43**, 1737 (1997).

Besnoin, J.-M., and K. Y. Choi, "Identification and Characterization of Reaction Byproducts in the Polymerization of Polyethylene Terephthalate," *J. Macromol. Sci.—Rev. Macromol. Chem. Phys.*, **C29**(1), 55 (1989).

Besnoin, J.-M., G. D. Lei, and K. Y. Choi, "Melt Transesterification of Dimethyl Terephthalate with Ethylene Glycol," *AIChE J.*, **35**, 1445 (1989).

Bhatia, K. K., "Continuous Polyester Process," U.S. Patent No. 5,434,239 (July 18, 1995).

Choi, B. R., and H. H. Lee, "Transient and Steady-State Behavior of Wiped-Film Reactors for Reversible Condensation Polymerization," *Ind. Eng. Chem. Res.*, **35**, 1550 (1996).

Choi, K. Y., "A Modeling of Semibatch Reactors for Melt Transesterification of Dimethyl Terephthalate with Ethylene Glycol," *Poly. Eng. Sci.*, **27**, 1703 (1987).

Dotson, N. A., R. Galvan, R. L. Laurence, and M. Tirrell, *Polymerization Process Modeling*, VCH Publishers, New York (1996).

Douglas, J. M., *Conceptual Design of Chemical Processes*, McGraw-Hill, New York (1988).

Gupta, S. K., and A. Kumar, *Reaction Engineering of Step Growth Polymerization*, Plenum Press, New York (1987).

Giudici, R., C. A. O. do Nascimento, I. C. Beiler, and N. Scherbakoff, "Transient Experiments and Mathematical Modeling of an Industrial Twin-Screw Extruder Reactor for Nylon-6,6 Polymerization," *Ind. Eng. Chem. Res.*, **36**, 3513 (1997).

Jacobs, D. B., and J. Zimmerman, "Preparation of 6,6-Nylon and Related Polyamides," *Polymerization Processes*, C. E. Schildknecht and I. Skeist, eds., Wiley, New York (1977).

Jacobsen, L. L., and W. H. Ray, "Unified Modeling of Polycondensation Processes," *J. Macromol. Sci.—Rev. Macromol. Chem. Phys.*, **C32**, 407 (1992a).

Jacobsen, L. L., and W. H. Ray, "Analysis and Design of Melt and Solution Polycondensation Processes," *AIChE J.*, **38**, 911 (1992b).

Jaswal, I., and K. Pugi, "Preparation of Polyamides by Continuous Polymerization," U.S. Patent No. 3,900,450 (Aug. 19, 1975).

Katz, M., "Preparation of Linear Saturated Polyesters," *Polymerization Processes*, C. E. Schildknecht and I. Skeist, eds., Wiley, New York (1977).

Kemkes, J. F., "Direct Esterification of Terephthalic Acid with Ethylene Glycol Under Atmospheric Pressure," *J. Poly. Sci.: Part C*, **22**, 713 (1969).

Kumar, A., S. Kuruville, A. R. Raman, and S. K. Gupta, "Simulation of Reversible Nylon-6,6 Polymerization," *Polymer*, **22**, 387 (1981).

Kumar, A., R. K. Agarwal, and S. K. Gupta, "Simulation of Reversible Nylon-6,6 Polymerization in Homogeneous Continuous-Flow Stirred Tank Reactors," *J. Appl. Poly. Sci.*, **27**, 1759 (1982).

Nisoli, A., M. F. Malone, and M. F. Doherty, "Attainable Regions for Reaction with Separation," *AIChE J.*, **43**, 374 (1997).

Ravindranath, K., and R. A. Mashelkar, "Modelling of Polyethylene Terephthalate Reactors 1. A Semibatch Ester Interchange Reactor," *J. Appl. Poly. Sci.*, **26**, 3179 (1981).

Ravindranath, K., and R. A. Mashelkar, "Modelling of Polyethylene Terephthalate Reactors 2. A Continuous Transesterification Process," *J. Appl. Poly. Sci.*, **27**, 471 (1982a).

Ravindranath, K., and R. A. Mashelkar, "Modelling of Polyethylene Terephthalate Reactors 3. A Semibatch Prepolymerization Process," *J. Appl. Poly. Sci.*, **27**, 2625 (1982b).

Ravindranath, K., and R. A. Mashelkar, "Modelling of Polyethylene Terephthalate Reactors 4. A Continuous Esterification Process," *Poly. Eng. Sci.*, **22**, 610 (1982c).

Ravindranath, K., and R. A. Mashelkar, "Polyethylene Terephthalate—I. Chemistry, Thermodynamics, and Transport Properties," *Chem. Eng. Sci.*, **41**, 2197 (1986a).

Ravindranath, K., and R. A. Mashelkar, "Polyethylene Terephthalate—II. Engineering Analysis," *Chem. Eng. Sci.*, **41**, 2969 (1986b).

Samant, K. D., and K. M. Ng, "Synthesis of Extractive Reaction Processes," *AIChE J.*, **44**, 1363 (1998a).

Samant, K. D., and K. M. Ng, "Effect of Kinetics and Mass Transfer on Design of Extractive Reaction Processes," *AIChE J.*, **44**, 2212 (1998b).

Sauerbrunn, R. D., "Diamine Recovery Process," U.S. Patent No. 4,380,615 (Apr. 19, 1983).

Schaeffer, M. N., "Process for Esterification," U.S. Patent No. 5,476,919 (Dec. 19, 1995).

Steppan, D. D., "The Design of Continuous Polycondensation Reactors," PhD Thesis, Univ. of Massachusetts, Amherst (1989).

Ung, S., and M. F. Doherty, "Vapor-Liquid Phase Equilibrium in Systems with Multiple Chemical Reactions," *Chem. Eng. Sci.*, **50**, 23 (1995a).

Ung, S., and M. F. Doherty, "Synthesis of Reactive Distillation Systems with Multiple Equilibrium Chemical Reactions," *Ind. Eng. Chem. Res.*, **34**, 2555 (1995b).

Ung, S., and M. F. Doherty, "Necessary and Sufficient Conditions for Reactive Azeotropes in Multireaction Mixtures," *AIChE J.*, **41**, 2383 (1995c).

Venimadhavan, G., G. Buzad, M. F. Doherty, and M. F. Malone, "Effect of Kinetics on Residue Curve Maps for Reactive Distillation," *AIChE J.*, **40**, 1814 (1994).

Vodonik, J. L., "Continuous Ester Interchange Process," U.S. Patent No. 2,829,153 (Apr. 1, 1958).

Vrentas, J. S., J. L. Duda, and S. T. Hsieh, "Thermodynamic Properties of Some Amorphous Polymer-Solvent Systems," *Ind. Eng. Chem. Prod. Res. Dev.*, **22**, 326 (1983).

Appendix: Reactive Azeotropes, Residue Curve Maps, and Distillation Boundaries for Polycondensation Systems

The necessary and sufficient condition for azeotropy in a vapor-liquid multicomponent reactive system is given by (Ung and Doherty, 1995c)

$$X_i = Y_i, \qquad i = 1,2,\ldots,c-r-1, \tag{A1}$$

where X_i and Y_i are transformed mole fractions of component i in liquid and vapor phase, respectively.

Let us consider the system of Example 1 in more detail. The system comprises five apparent components, viz., EG, M, Z, E_m, and E_g, of which only EG and M are volatile. The polymeric components Z, E_m, and E_g are nonvolatile and can exist only in the liquid phase. Hence the vapor phase is constrained to lie on the EG–M edge of the reactive phase diagram (see Figure 2), that is,

$$Y_i = 0, \qquad \forall T, P, \qquad i = Z, E_m, E_g. \tag{A2}$$

In the context of Eq. A2, the only region of the reactive phase diagram where Eq. A1 can possibly be satisfied is the EG–M edge. As this edge represents a nonreactive binary mixture of EG and methanol, it can easily be shown that the condition of Eq. A1 translates to the condition of azeotropy for the binary EG–M mixture (Eq. A3):

$$\begin{aligned} x_i = y_i, &\quad i = \text{EG, M} \\ x_i = y_i = 0, &\quad i = Z, E_m, E_g. \end{aligned} \tag{A3}$$

Thus the only azeotrope the reactive system can possess is a binary azeotrope between EG and methanol. The EG–M mixture is decidedly nonideal, but does not possess any azeotrope. Hence we expect the reactive system to be free of azeotropes. The absence of azeotropes also suggests that there are no reactive distillation boundaries. This is indeed confirmed by the residue curve map (for $P = 1$ atm) shown in Figure 2.

Using the same arguments, we can show that the only azeotropes the systems of Examples 2 and 3 can possess are the nonreactive binary azeotropes between EG and water, and HMDA and water, respectively. As the EG–W, and HMDA–W mixtures do not possess a binary azeotrope, the reactive systems of Examples 2 and 3 are also free from azeotropes and distillation boundaries. These observations also have been verified, but not shown here for the sake of brevity.

Note that this analysis is valid only for a vapor-liquid system. It can still be used for Example 2, however, as we use a reactive distillation column only when the solid phase has completely disappeared. Also note that the assumption of polymeric species being nonvolatile is sufficiently accurate over the range of temperatures and pressures typically used. Any component that is sufficiently volatile has to be considered as a separate component in the VLE model, the kinetic scheme, and rate expressions.

Manuscript received Oct. 20, 1998, and revision received Apr. 28, 1999.